Isthminia panamensis, a new fossil inioid (Mammalia, Cetacea) from the Chagres Formation of Panama and the evolution of 'river dolphins' in the Americas

Nicholas D. Pyenson[1,2], Jorge Vélez-Juarbe[3,4], Carolina S. Gutstein[1,5], Holly Little[1], Dioselina Vigil[6] and Aaron O'Dea[6]

[1] Department of Paleobiology, National Museum of Natural History, Smithsonian Institution, Washington, DC, USA
[2] Departments of Mammalogy and Paleontology, Burke Museum of Natural History and Culture, Seattle, WA, USA
[3] Department of Mammalogy, Natural History Museum of Los Angeles County, Los Angeles, CA, USA
[4] Florida Museum of Natural History, University of Florida, Gainesville, FL, USA
[5] Comisión de Patrimonio Natural, Consejo de Monumentos Nacionales, Santiago, Chile
[6] Smithsonian Tropical Research Institute, Balboa, Republic of Panama

ABSTRACT

In contrast to dominant mode of ecological transition in the evolution of marine mammals, different lineages of toothed whales (Odontoceti) have repeatedly invaded freshwater ecosystems during the Cenozoic era. The so-called 'river dolphins' are now recognized as independent lineages that converged on similar morphological specializations (e.g., longirostry). In South America, the two endemic 'river dolphin' lineages form a clade (Inioidea), with closely related fossil inioids from marine rock units in the South Pacific and North Atlantic oceans. Here we describe a new genus and species of fossil inioid, *Isthminia panamensis*, gen. et sp. nov. from the late Miocene of Panama. The type and only known specimen consists of a partial skull, mandibles, isolated teeth, a right scapula, and carpal elements recovered from the Piña Facies of the Chagres Formation, along the Caribbean coast of Panama. Sedimentological and associated fauna from the Piña Facies point to fully marine conditions with high planktonic productivity about 6.1–5.8 million years ago (Messinian), pre-dating the final closure of the Isthmus of Panama. Along with ecomorphological data, we propose that *Isthminia* was primarily a marine inhabitant, similar to modern oceanic delphinoids. Phylogenetic analysis of fossil and living inioids, including new codings for *Ischyrorhynchus*, an enigmatic taxon from the late Miocene of Argentina, places *Isthminia* as the sister taxon to *Inia*, in a broader clade that includes *Ischyrorhynchus* and *Meherrinia*, a North American fossil inioid. This phylogenetic hypothesis complicates the possible scenarios for the freshwater invasion of the Amazon River system by stem relatives of *Inia*, but it remains consistent with a broader marine ancestry for Inioidea. Based on the fossil record of this group, along with *Isthminia*, we propose that a marine ancestor of *Inia* invaded Amazonia during late Miocene eustatic sea-level highs.

Submitted 27 April 2015
Accepted 13 August 2015
Published 1 September 2015

Corresponding author
Nicholas D. Pyenson,
pyensonn@si.edu

Academic editor
Mark Young

Additional Information and Declarations can be found on page 40

DOI **10.7717/peerj.1227**

Subjects Ecology, Evolutionary Studies, Marine Biology, Paleontology, Zoology
Keywords River dolphins, Cetacea, Panama, Fossil record, Evolution, Neogene, Inioidea, Amazonia

INTRODUCTION

In the evolution of marine mammals, the dominant mode of their ecological transitions (*sensu* *Vermeij & Dudley, 2000*) is the iterative adaptation to marine life from terrestrial ancestry (*Thewissen & Williams, 2002*; *Gingerich, 2005*; *Kelley & Pyenson, 2015*). However, the direction of this ecological transition is not exclusively from land to sea: throughout the late Cenozoic, several lineages of cetaceans and pinnipeds have evolved exclusively freshwater lifestyles from a marine ancestry (*Hamilton et al., 2001*; *Pyenson, Kelley & Parham, 2014*). Among cetaceans, the group of extant 'river dolphins' are the best exemplars of this ecological mode. This non-monophyletic (i.e., paraphyletic or possibly polyphyletic) group traditionally includes four different living species: *Platanista gangetica* (*Lebeck, 1801*); *Lipotes vexillifer* *Miller, 1918*, *Inia geoffrensis* (*Blainville, 1817*), and *Pontoporia blainvillei* (*Gervais & d'Orbigny, 1844*). These species all show broad morphological similarities, including longirostral skulls and jaws, reduced orbits, flexible necks, and broad, paddle-shaped flippers (*Geisler et al., 2011*). Notably, this assemblage of broadly convergent taxa has a biogeographic distribution across different freshwater river systems of South Asia and South America, and in estuarine and coastal waters of the latter as well.

While work for most of 20th century implied or proposed that the 'river dolphins' were all most closely related to one another (e.g., *Simpson, 1945*), the advent of molecular phylogenies clarified that these lineages are not all directly related to one another (see *Geisler et al., 2011* for a useful summary), although both molecular and morphological analyses consistently group the two South American genera, *Inia* and *Pontoporia*, as sister taxa (Inioidea *sensu* *Muizon, 1988a*). *Lipotes*, which was endemic to the Yangtze River of China and is likely extinct (*Turvey et al., 2010*), may be the sister taxon to Inioidea (see *Geisler et al., 2011*), although all molecular studies (e.g., *Messenger & McGuire, 1998*; *Hamilton et al., 2001*; *Nikaido et al., 2001*; *Geisler & Sanders, 2003*; *Arnason, Gullberg & Janke, 2004*; *May-Collado & Agnarsson, 2006*; *McGowen, Spaulding & Gatesy, 2009*; *Steeman et al., 2009*; *Geisler et al., 2011*) and combined molecular and morphological analyses (*Geisler et al., 2011*; *Gatesy et al., 2013*) place *Lipotes* within Delphinida (i.e., Inioidea + Delphinoidea *sensu* *Muizon, 1988a*), and furthermore place *Platanista* outside of Delphinida. *Lipotes* and *Platanista* have only been grouped together in analyses using purely morphological datasets (e.g., *Geisler & Sanders, 2003*).

With restricted distributions, serious conservation threats, and relatively low taxonomic richness compared with other odontocete clades, the evolutionary history of 'river dolphins' remains a topic of perennial interest (*Cassens et al., 2000*; *Hamilton et al., 2001*; *Nikaido et al., 2001*; *Pyenson, 2009*; *Ruiz-Garcia & Shostell, 2010*; *Turvey et al., 2010*; *Geisler et al., 2011*). The fossil record of South Asian 'river dolphins' is poor, with no taxa reported from undisputable remains (e.g., *Prolipotes yujiangensis* *Zhou, Zhou & Zhao, 1984* is known only from an isolated mandible that cannot be clearly diagnosed). By

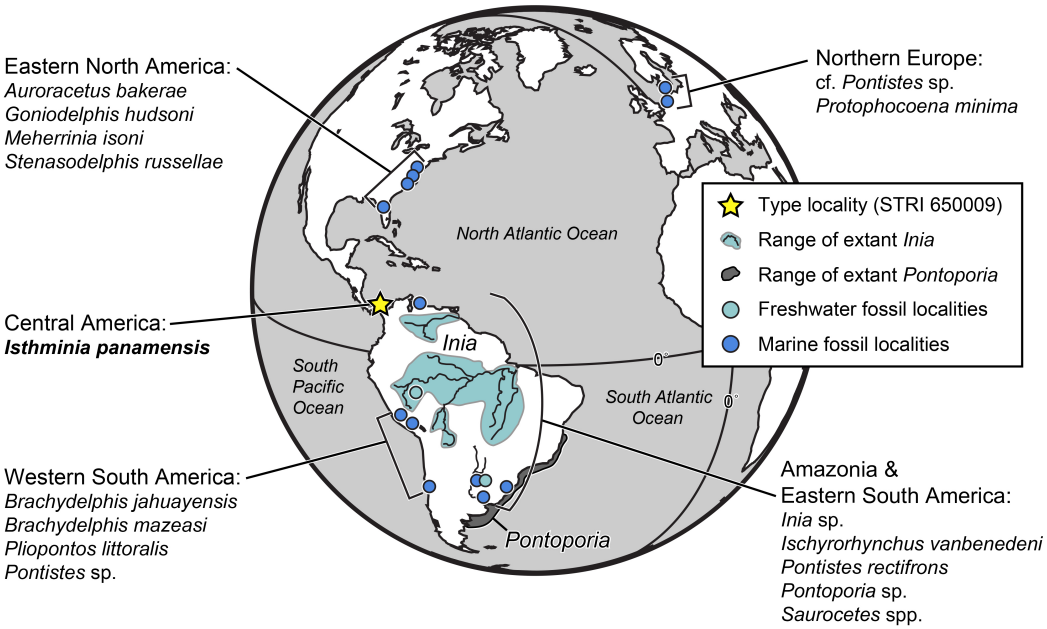

Figure 1 Map of fossil and living Inioidea. Global map of living and fossil inioids, projected onto an orthographic globe, centered on 15°N, 45°W. Extant distributions of *Inia geoffrensis* (teal and black waterways) and *Pontoporia blainvillei* (dark gray), follow data from the *IUCN (International Union for Conservation of Nature) (2013)* and *Secchi, Ott & Danilewicz (2003)*, respectively. Occurrences for fossil data derive from location of type localities for each taxon, except for reports for the Northern Europe by *Pyenson & Hoch (2007)*, Western South America by *Gutstein et al. (2015)*, and Amazonia and Eastern South America by *Cozzuol (2010)*. Major fossil localites for enumerated inioids identified at least to the generic level, are listed alphabetically by region, and represented by teal or blue dots, for freshwater and marine deposits, respectively. Base map generated by Indiemapper (http://indiemapper.com).

contrast, fossil South American 'river dolphins' have been reported from Neogene rocks of the continent since the 1850s (*Cozzuol, 1996*). The majority of these fossil taxa have been assigned to the traditional taxonomic groups of either Iniidae or Pontoporiidae, based on diagnostic features of the face and vertex (*Muizon, 1988a*), and include taxa (e.g., *Pontistes rectifrons Burmeister, 1885*, *Pliopontos littoralis Muizon, 1983*, *Brachydelphis mazeasi Muizon, 1988b*) known from marine rocks units of middle Miocene through Early Pliocene age in Argentina, Peru, Chile, and elsewhere (*Muizon, 1984*; *Muizon, 1988b*; *Cozzuol, 1996*; *Gutstein et al., 2009*; *Lambert & de Muizon, 2013*; *Gutstein et al., 2014a*). Recently, *Bianucci et al. (2013)* reported an isolated periotic with diagnostic features of Platanistinae (today limited to South Asia) from the Peruvian Amazon Basin of Laventan South American Land Mammal Age. This finding is striking for its disjunct biogeographic occurrence, relative to living *Platanista* in South Asia, but it is consistent with the widespread distribution of fossil platanistoids reported elsewhere in the world from late Paleogene through Neogene rocks along the coasts of the South and North Pacific and the North Atlantic oceans (*Fordyce, 2009*).

Similarly, the fossil record of inioids extends well beyond South America (Fig. 1). Fossil pontoporiids have been described from shallow marine and estuarine strata of early late Miocene to Early Pliocene age from the Atlantic coast of North America, including

Maryland, Virginia, North Carolina and Florida (*Morgan, 1994*; *Whitmore, 1994*; *Godfrey & Barnes, 2008*; *Gibson & Geisler, 2009*; *Geisler, Godfrey & Lambert, 2012*). Along the Atlantic coast of Europe, *Protophocaena minima* *Abel, 1905* from shallow marine Miocene of the Netherlands, is now recognized as a pontoporiid (*Lambert & Post, 2005*) based on additional cranial and periotic material from the Miocene of Belgium and the Netherlands. *Pyenson & Hoch (2007)* reported pontoporiids (cf. *Pontistes* sp. and indeterminate Pontoporiidae) from the marine Gram Formation in Denmark, which is early late Miocene age. To date, no fossil pontoporiids have been described from the North Pacific Ocean. The two species of *Parapontoporia* *Barnes, 1984*, which are well known from abundant Mio-Pliocene localities in northern and southern California (*Boessenecker & Poust, 2015*), are not pontoporiids, but belong in a clade with *Lipotes* (*Geisler, Godfrey & Lambert, 2012*), although *Parapontoporia* is sometimes also grouped with *Platanista, Lipotes* and *Ischyrorhynchus vanbenedeni* *Ameghino, 1891* (see *Aguirre-Fernández & Fordyce, 2014*). Historically, fossils referred to Iniidae include a variety of taxa (e.g., *Goniodelphis hudsoni* *Allen, 1941*; *Ischyrorhynchus*), supplementing the existing data showing a much broader geographic extent for inioids in the fossil record than today (Fig. 1). These fossil occurrences thus raise the question of how Inioidea evolved, and the evolutionary scenarios that led to their current distribution. Our description herein of a new genus and new species of Inioidea from the late Miocene of Panama, based on substantially more osteological material than most fossil inioids, provides new insight into the evolutionary scenarios under which this group evolved in South America, including the timing and mode of major ecological transitions.

METHODS

Excavation at the type locality

The type specimen of this new taxon was initially discovered in an intertidal zone outcrop of the Chagres Formation, near the town of Piña, along the Caribbean coastline of Panama, in early 2011 (Fig. 2 and Fig. S1). The infrequency of low tides at the type locality created a narrow time window for excavating the specimen, which several co-authors (NDP, JVJ, DV, and AO) undertook on 18 June 2011 with the assistance of staff from Smithsonian Tropical Research Institute (STRI). After exporting the specimen under permits from Panama's Ministerio de Comercio e Industrias (MICI number DNRM-MC-074-11) to the Smithsonian's National Museum of Natural History (NMNH) in Washington, D.C., USA, the specimen was prepared using mechanical tools and consolidated using standard fossil vertebrate preparation techniques by DV, S Jabo, and P Kroehler in the Vertebrate Paleontology Preparation Laboratory in the Department of Paleobiology at NMNH.

Digital methods

During excavation at the type locality (Fig. S1), we documented *in situ* skeletal remains using a Flip camera (Cisco Systems Inc., San Jose, California, USA) on time-lapse settings. Later, subsequent to the specimen's preparation in the Department of Paleobiology, we used computed tomography (CT) to scan the type specimen USNM 546125 in the

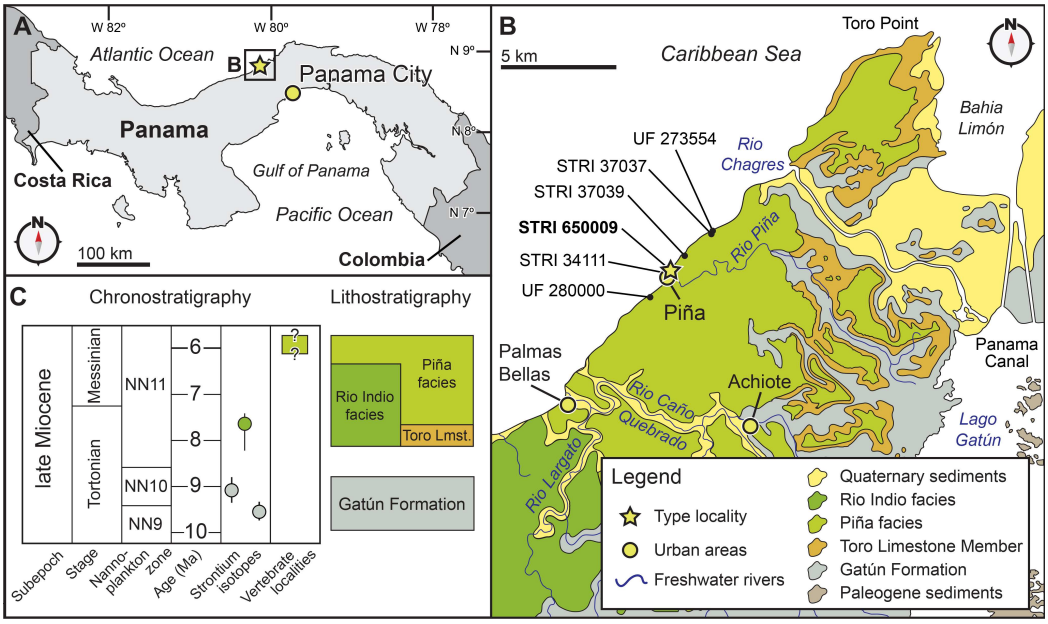

Figure 2 Locality and geology. Geographic and stratigraphic context of *Isthminia panamensis*. (A) Map of Central America with a yellow star representing the type locality, STRI locality 650009. (B) Map of north-central Panama with the distribution of the Chagres Formation, with type locality of *Isthminia* in the vicinity of Piña, along with other fossil vertebrates. (C) Chronostratigraphic and lithostratigraphic relationships of the Chagres Formation (modified from *Hendy et al., in press*, and *Velez-Juarbe et al., 2015*).

Department of Anthropology with a Siemens Somatom Emotion 6 at slice thickness of 0.63 mm (which results in a three-dimensional reconstruction increment of 0.30 mm). The resultant DICOM files were processed by loading image files in Mimics (Materialise NV, Leuven, Belgium), and a mask was created based on the threshold of bone, relative to the nominal density of air. We then created a three-dimensional (3D) object from this mask, and exported the resultant file as an ASCII STL, which was opened in Geomagic (ver. 2012) for final imaging edits. We also attempted to use laser surface scanning (i.e., laser arm scanner) to capture 3D data, but line of sight issues with overhanging morphological features and the geometric complexity of the type specimen prevented a full capture of the surface geometry. As a result, we elected to use the 3D models of the skull, mandibles, and scapula generated from CT data because this method provided complete capture of the external and internal morphology. After converting the CT files into 3D data, the watertight model was then processed in Autodesk Maya (ver. 2013) by Pixeldust Studios (Bethesda, Maryland, USA), decimating the models to 100,000 triangles and creating diffuse, normal, and occlusion texture maps. The resultant 3D surface model datasets, processed from the computed tomography scans, provided sub-millimeter accuracy, and full resolution files can be downloaded at the open-access Smithsonian X 3D browser (http://3d.si.edu). These files, along with supplemental ones, are also archived at Zenodo (http://zenodo.org) at the following DOI: 10.5281/zenodo.27214.

Phylogenetic analysis

Recent work on the systematics of living and extinct odontocetes has recently provided several phylogenetic frameworks to use in this study. *Geisler et al. (2011)* used a combined morphological and molecular analysis to clarify the relationships among extant and fossil lineages of cetaceans, with mostly a focus on odontocetes, including some important fossil taxa, but taxon sampling within Inioidea was relatively sparse compared to *Geisler, Godfrey & Lambert (2012)*. This latter work, which described *Meherinnia isoni Geisler, Godfrey & Lambert, 2012*, a late Miocene inioid from marine rocks of North Carolina, USA, also included other fossil inioids such as *Auroracetus bakerae Gibson & Geisler, 2009*, *Ischyrorhynchus vanbenedeni Ameghino, 1891*, *Protophocaena minima*, and *Stenasodelphis russellae Godfrey & Barnes, 2008*, some of which were not included in subsequent phylogenetic analyses of odontocetes, such as the one by *Murakami et al. (2014)*. The starting point for our analysis was the matrix provided by *Aguirre-Fernández & Fordyce (2014)* in their description of the early Miocene stem odontocete *Papahu taitapu Aguirre-Fernández & Fordyce, 2014*, which used the morphological partition of *Geisler, Godfrey & Lambert (2012)* in their description of *Meherrinia*, along with some important modifications (e.g., the removal of Mysticeti and unpublished specimens, and coding revisions for select stem odontocetes) that enhanced its utility for resolving fossil and living odontocete relationships.

We added *Isthminia* as an operational taxonomic unit to the *Aguirre-Fernández & Fordyce (2014)* matrix of 311 characters, and updated the character scoring for *Ischyrorhynchus*, which was the only inioid taxon not coded from direct observation in any previous study. The codings for *Ischyrorhynchus* herein were made by one of the authors of this study (CSG), who reviewed all the specimens in Argentina (e.g., MLP 5–16, MACN 15135), which resulted in modifications for 20 character codings (see File S1). The cladistic search was performed in PAUP* (*Swofford, 2002*) using all characters as unordered. We first performed a heuristic search using the tree bisection-reconnection (TBR) algorithm. In addition, we conducted statistical support analyses by searching for successively longer trees to calculate decay indices and 1,000 bootstrap replicates. The complete matrix is available in the Supplemental Information (see File S1).

Phylogenetic nomenclature

We followed the recommendations of *Joyce, Parham & Gauthier (2004)* for the conversion of select ranked taxonomic cetaceans names to phylogenetically defined ones in this study. The taxonomy of marine mammals includes several extant monospecific forms in their own familial rank, such as *Eschrichtius robustus* (*Lilljeborg, 1861*), *Physeter macrocephalus Linnaeus, 1758*, *Pontoporia blainvillei*, or *Lipotes vexillifer*. In many of these latter cases, the conceptual basis for the higher taxonomic rank includes many fossil taxa that connect the monospecific taxon to their nearest living relatives, especially with stem lineages that range into geologic times that remain poorly sampled and known (e.g., the Oligocene; see *Uhen & Pyenson, 2007*). While it would be ideal to create stem-based clade names for these single species, there remains no pathway to define pan-stems

based on single species, even more than 10 years after *Joyce, Parham & Gauthier (2004)*'s recommendations. Here we follow *Joyce, Parham & Gauthier (2004)*'s logic in the specific case of the pan-stem for the lineage leading to extant *Inia*, by forming a new pan-stem name by combining the current Linnaean generic name with the prefix 'pan,' and then referred traditional family names to a more inclusive clade whose composition closely resembles our current name application. For these purposes, we used abbreviations NCN for New Clade Name and CCN for Converted Clade Name. Below, we clarify our precise definitions for these clades (see PhyloCode, 2014, Article 9.3; *Cantino & de Queiroz, 2014*), and we also provide full citations for the names of specifier species.

Specimens observed

Auroracetus bakerae (USNM 534002), *Inia geoffrensis* (USNM 395415, 49582, 239667), *Ischyrorhynchus vanbenedeni* (MACN 15135, MLP 5–16), *Lipotes vexillifer* (USNM 218293, AMNH 57333), *Meherrinia isoni* (CMM-V-4051, USNM 559343, identified by JA Geisler), *Pontoporia blainvillei* (USNM 482727, 482771, 482707), *Stenasodelphis russellae* (CMM-V-2234).

Nomenclatural acts

The electronic version of this article in Portable Document Format (PDF) will represent a published work according to the International Commission on Zoological Nomenclature (ICZN), and hence the new names contained in the electronic version are effectively published under that Code from the electronic edition alone. This published work and the nomenclatural acts it contains have been registered in ZooBank, the online registration system for the ICZN. The ZooBank LSIDs (Life Science Identifiers) can be resolved and the associated information viewed through any standard web browser by appending the LSID to the prefix http://zoobank.org/. The LSID for this publication is: urn:lsid:zoobank.org:pub:4763A625-883D-4263-B376-33B9F9AD56A4. The online version of this work is archived and available from the following digital repositories: PeerJ, PubMed Central and CLOCKSS.

RESULTS

Systematic paleontology

Cetacea *Brisson, 1762*
Odontoceti *Flower, 1867*
Delphinida *Muizon, 1988a*
Inioidea *Gray, 1846 sensu Muizon, 1988a*
Pan-Inia (NCN) (panstem-based version of *Inia* (Blainville, 1817))
Isthminia, gen. nov. LSID: urn:lsid:zoobank.org:act:83F6A9B4-289D-45DE-A3D1-C361DAAAF973.

Definitions '*Pan-Inia*' refers to the panstem that includes crown *Inia* (CCN), and all other lineages closer to *Inia* than to *Pontoporia*, such as *Isthminia* and *Ischyrorhynchus*. Subjective

synonymies of *Pan-Inia* include: Iniidae *Gray, 1846*; Iniinae *Flower, 1867*; Saurocetidae *Ameghino, 1891*; Iniidae *Muizon, 1984*; Ischyrorhynchinae (*Cozzuol, 1996*); Iniidae *Cozzuol, 2010*; Iniidae *Gutstein, Cozzuol & Pyenson, 2014b*. Crown group *Inia* refers to the crown clade arising from the last common ancestor of all named species of *Inia*, including *Inia boliviensis d'Orbigny, 1834* and *Inia araguaiaensis Hrbek et al., 2014*. Although we follow the suggestions of the Society for Marine Mammalogy's Committee on Taxonomy (2014) in provisionally recognizing two sub-species of *Inia geoffrensis* (*I. g. geoffrensis* and *I.g. humboldtiana Pilleri & Gihr, 1977*), the phylogenetic definition of *Inia* can accommodate a plurality of species and subspecies.

Type and only known species. *Isthminia panamensis*, sp. nov.

Etymology. *Isthm-* reflects the type specimen's provenance from the Isthmus of Panama and the crucial role that the formation of this isthmus played in Earth history and evolution of the biota of the Americas. This epithet follows in the tradition of another fossil cetacean from the Chagres Formation, *Nanokogia isthmia Velez-Juarbe et al., 2015*. The feminine generic epithet *Inia* reflects its similarities to the living Amazon River dolphin (*Inia geoffrensis*). Pronunciation: 'Ist-min-ee-a,' with the emphasis on the second syllable.

Age. Same as that of the species.

Diagnosis. Same as that of the species.

Isthminia panamensis sp. nov. (Figs. 3–12 and Tables 1–3)

LSID: urn:lsid:zoobank.org:act:A5C706B6-E0B6-43E5-A65C-E6FE0B2BDF1A

Holotype. USNM 546125, consisting of an incomplete skull, both right and left mandibles, an incomplete right scapula, and two carpals. The skull lacks the basicranium and tympanoperiotics. The holotype was collected by several of the co-authors of this study (NDP, JVJ, DV, and AO), with assistance from staff from STRI, in 2011.

Type locality. STRI locality 650009 (9°16′55.4880″N, 80°02′49.9200″W), less than 100 m northeast of the main road in the town of Piña, along the Caribbean Sea coastline of the Republic of Panama (Fig. 2).

Formation. Piña Facies of the Chagres Formation.

Age. Microfossils place the Chagres Formation in calcareous nanofossil zone NN11 and planktonic foraminiferal zones M13b-M14, suggesting an age range between 8.52 to 5.57 Ma, i.e., Tortonian to Messinian in age (*Collins et al., 1996*). *Hendy et al. (in press)* obtained a Sr date of ∼7.64 Ma from a single mollusc shell that was collected stratigraphically below the unit where the type specimen of *Isthminia* was discovered. This result, however, conflicts with planktonic foraminiferal data. The top of the Toro Point Member of the Chagres Formation includes co-occurring *Globorotalia margaritae Bolli & Bermúdez, 1965* and *G. lenguaensis Bolli, 1957*. *Collins et al. (1996)* indicating an astronomically calibrated age (*Wade et al., 2011*) of 6.13–6.08 Ma. *Globoquadrina dehiscens Chapman, Parr & Collins, 1934* has an age range of 23.2–5.8 Ma (*Wade et al., 2011*) and occurs throughout the stratigraphic section, including Panama Paleontology Project locality (PPP) 1099 (*Collins et al., 1996*), which is located less than 1 kilometer from STRI locality 650009, and coeval with the type specimen of *Isthminia*. Because the Piña Facies is stratigraphically above the

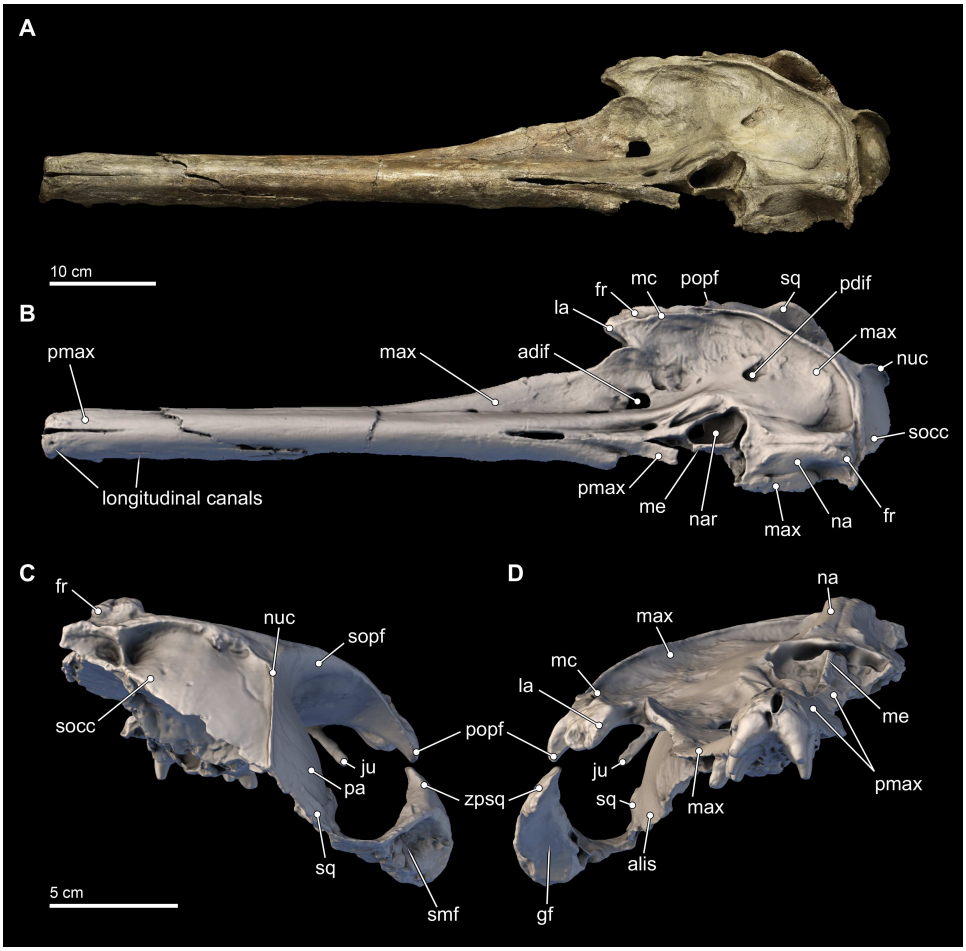

Figure 3 Skull in dorsal, anterior, and posterior views. Dorsal views of the type skull of *Isthminia panamensis* (USNM 546125) from (A) photographs and (B) orthogonal digital three-dimensional polygon model prepared from CT data, with lighting and color modifications using the Smithsonian X 3D browser. (C) Anterior and (D) posterior views of the type skull of *Isthminia panamensis* (USNM 546125) from orthogonal digital three-dimensional polygon model prepared from CT data. See http://3d.si.edu/explorer?s=h2mqJ9 (dorsal view), http://3d.si.edu/explorer?s=bA5gJO (posterior view), and http://3d.si.edu/explorer?s=e1seD5 (anterior view) to measure, modify, or download this model.

Toro Member in the Chagres Formation, these observations therefore constrain the age of the type specimen of *Isthminia* to 6.1–5.8 Ma (Messinian).

Diagnosis. *Isthminia* is a medium sized crown odontocete (approximately 285 cm in total length), which can be can differentiated from all other odontocetes by the following combination of character states. First, *Isthminia* belongs in Inioidea based on: the presence of a very long mandibular symphysis (c. 39[2]); a fused mandibular symphysis (c. 40[0]); a lacrimal that wraps around anterior edge of supraorbital process of frontal and slightly overlies its anterior end (c. 51[1]); and the maxilla forming the dorsolateral edge of the ventral infraorbital foramen (c. 57[1]).

Isthminia is characterized by the following unique combination of character states among Inioidea: rostral constriction well anterior to antorbital notch (c. 6[1]), shared

Table 1 **Measurements of holotype skull and mandibles (USNM 546125) of *Isthminia panamensis*, in mm (modified after *Perrin, 1975* and *Tanaka & Fordyce, 2014*).**

	Measurement (mm)
Skull	
Total length from the most anterior point to the posterior most point	571+
Cranial length	185+
Length of rostrum—from tip to line across hindmost limits of antorbital notches	381
Width of rostrum at base—along line across hindmost limits of antorbital notches	124*
Width of rostrum at 60 mm anterior to line across hindmost limits of antorbital notches	90*
Width of rostrum at mid-length	36+
Width of premaxillae at mid-length of rostrum	31+
Width of rostrum at 3/4 length, measured from posterior end	50*
Greatest width of premaxillae	78*
Projection of premaxillae beyond maxillae measured from tip of rostrum to line across foremost tips of maxillae visible in dorsal view	85+
Width of premaxillae at a line across posterior limits of antorbital notches	48*
Maximum width of premaxillae at mid-orbit level	52*
Preorbital width at level of frontal-lacrimal suture	184*
Postorbital width across apices of postorbital processes	232*
Distance from tip of rostrum to external nares (to mesial end of anterior transverse margin of right naris)	419+
Distance from foremost end of junction between nasals to hindmost point of margin of supraoccipital crest	68
Greatest width of external nares	49
Median length of the nasals	58
Maximum length of the right nasal	58
Median length of frontals on the vertex	25
Vertical external height of the skull from ventral most braincase to dorsal extremity of vertex	150+
Bizygomatic width	262*
Length of upper left tooth row—from hindmost margin of hindmost alveolus to tip of rostrum	329
Number of teeth—upper left	18
Number of teeth—upper right	18
Mandible	
Maximum preserved length of left mandible	478+
Maximum preserved height of left mandible	74+
Number of teeth—lower left	17
Number of teeth—lower right	18
Length of the lower tooth row from tip of mandible to posterior margin of posterior most alveolus	315

Notes.
Asterisk indicates doubling of measurement from one side. Positive sign indicates preserved distance.

with *Pontoporia*; posterior edge of rostral edge bowed forming a deep U-shaped antorbital notch (c. 11[2]), shared with *Brachydelphis* spp.; small transverse distance between lateral edges of left and right premaxillae at antorbital notch (c. 66[0]), shared with *Auroracetus* and *Inia*; short posterolateral sulcus (c. 72[1]), shared with *Protophocoena*, *Stenasodelphis*, and *Auroracetus*; thickened anterolateral corner of maxilla over supraorbital process of frontal (c. 78[1]), shared with *Pontoporia* and *Stenasodelphis*; presence of a maxillary

Table 2 Measurements of the scapula (USNM 546125) of *Isthminia panamensis*, in mm (modified after *Perrin, 1975*).

Scapula	Measurement (mm)
Maximum height of scapula	141+
Height of scapula from posterior margin of glenoid fossa to glenovertebral angle	161
Length of coracoid process	40
Greatest width of coracoid process	23
Greatest width of acromion process	26

Table 3 Relative orbit size (ROS) in *Isthminia panamensis*, and in other fossil and modern odontocetes, ranked in increasing value.

Genus	Species	Specimen	ROS	Source
Aulophyseter	*morricei*	LACM 154100, USNM 11230	0.20	This study (average, $n = 2$)
Orycterocetus	*crocodilinus*	USNM 22926	0.22	This study
Inia	*geoffrensis*	USNM 23967, 49582, 395415	0.24	This study (average, $n = 3$)
Lipotes	*vexillifer*	USNM 218293	0.32	This study
Aprixokogia	*kelloggi*	USNM 187015	0.34	This study
Lophocetus	*repenningi*	USNM 23886	0.36	This study
Simocetus	*rayi*	USNM 356517	0.36	This study
Isthminia	***panamensis***	**USNM 546125**	**0.40**	**This study**
Nanokogia	*isthmia*	UF 280000	0.40	*Velez-Juarbe et al., 2015*
Xiphiacetus	*bossi*	USNM 8842, 175381	0.42	This study (average, $n = 2$)
Delphinodon	*dividum*	USNM 7278	0.46	This study
Kogia	*sima*	LACM 47142	0.55	This study
Meherrinia	*isoni*	IRSNB M.2013	0.56	*Geisler, Godfrey & Lambert, 2012*
Pontoporia	*blainvillei*	USNM 482707, 482717, 482771	0.57	This study (average, $n = 3$)
Atocetus	*nasalis*	LACM 30093	0.58	*Barnes, 1985a*
Kentriodon	*pernix*	USNM 8060	0.58	This study
Parapontoporia	*wilsoni*	UCMP 83790	0.62	*Barnes, 1985b*
Brachydelphis	*jahuayensis*	MNHN PPI 267, 268; MUSM 567, 568	0.70	*Lambert & de Muizon, 2013* (average, $n = 4$)
Brachydelphis	*mazeasi*	MNHN PPI 121, 266; MUSM 564	0.80	*Lambert & de Muizon, 2013* (average, $n = 3$)

ridge (c. 79[1]), shared with *Brachydelphis mazeasi*; V-shaped anterior edge of nasal opening (c. 81[0]), shared with *Protophocoena* and *Auroracetus*; posterior end of premaxilla adjacent to lateral edge of nasal opening (c. 89[0]), shared with *Brachydelphis* spp.; suture with left and right nasals and right and left frontals shifted towards the left (c. 114[1]), shared with *Pliopontos* and *Inia*; nasals that are anteroposteriorly elongated (c. 117[0]), shared with all inioids except *Ischyrorhynchus* and *Inia*; supraoccipital below frontal and/or nasals (c. 128[0]), shared with *Protophocoena*, *Meherrinia* and *Ischyrorhynchus*; dorsal margin of mesethmoid at same level of premaxilla (c. 305[1]), shared with *Brachydelphis mazeasi* and *Stenasodelphis*; intermediate separation between posterior-most point of right premaxilla and nasal (c. 306[1]), shared with *Pontoporia* and *Stenasodelphis*; medial portion of maxilla on either side of the vertex face mainly dorsally (c. 307[2]), shared with

Pontoporia and *Pliopontos*; longest side of nasal facing anterodorsally (c. 311[1]), shared with all inioids except *Pontoporia* (face dorsally: c. 311[0]), and *Ischyrorhynchus* and *Inia* (face anteriorly: c. 311[2]).

Among other fossil inioids in the panstem to *Inia*, *Isthminia* shares the following: with *Meherrinia* and *Inia* (not preserved in *Ischyrorhynchus*) three or more dorsal infraorbital foramina (c. 64[2]); with *Ischyrorhynchus*, premaxillae on anterior two thirds of rostrum contact along the midline for nearly their entire length (c. 9[0]), tooth enamel with reticular striae (c. 26[1]), and anterior edge of nasals in line with posterior half of supraorbital processes (c. 80[4]); with *Inia* and *Ischyrorhynchus* supraorbital processes of frontal that slope laterodorsally away from vertex (c. 46 [2]), transverse width of nasals within 10% of nares width (c. 119[2]), nasals elevated above rostrum relative to lateral edge of maxilla (c. 123[1]), and frontals higher than nasals (c. 124[2]); with *Inia* the following synapomorphies: posterior buccal teeth that are nearly an equilateral triangle (c. 30 [1]), small lacrimal (c. 50[0]), small exposure of the lacrimal and jugal posterior to the antorbital notch (c. 55[0]), posterior portion of nasals elevated above rostrum (c. 123[1]), frontals posterior to nasals with same width as nasals (c. 125[1]), maxilla on dorsal surface of skull does not contact supraoccipital posteriorly (c. 129[0]), and dorsal edge of zygomatic process with distinct dorsal flange (c. 143[1]).

Lastly, *Isthminia* displays the following apomorphies: maxilla and premaxilla fused along most of rostrum (c. 10[0]); lower number of mandibular teeth (18) (c. 37[5]); dorsal edge of orbit low relative to lateral edge of rostrum (c. 47[1]); premaxilla is convex transversely anterior to nasal openings (c. 68[1]); posterior-most end of ascending process of premaxilla in line with posterior half of supraorbital process of frontal (c. 74[2]); very narrow width of posterior edge of nasals (c. 120[3]); slight emargination of posterior edge of zygomatic process by sternomastoid muscle fossa (c. 144[1]); and dental roots that are elongate, rugose, bulbous, and much larger than the tooth crowns, with some roots that have their apices oriented posteriorly so that they come close to the anterior end of the root of the succeeding tooth.

Etymology. The species epithet recognizes the Republic of Panama, its people, and the many generations of scientists who have studied its geological and biological histories.

Description

Skull

The skull of *Isthminia* is relatively complete on its dorsal aspect, although it is missing the left side of the facial bones (Fig. 3). The skull is heavily eroded along its ventral surface, and the basicranium is absent except for a small portion of the right parietal and right alisphenoid (Fig. 4). The skull preserves most of the dorsal aspect of the supraoccipital, including small portions that articulate with the vertex and nuchal and sigmoidal crests (Figs. 3A–3C). Overall, the profile of the skull is dominated by the rostrum (Fig. 5), which is complete and comprises approximately 75% of the length of the preserved skull (the rostrum length is 36.6 cm; Table 1). The anterior portion of the rostrum is slightly displaced by both an oblique and transverse fractures, likely from geologic compaction

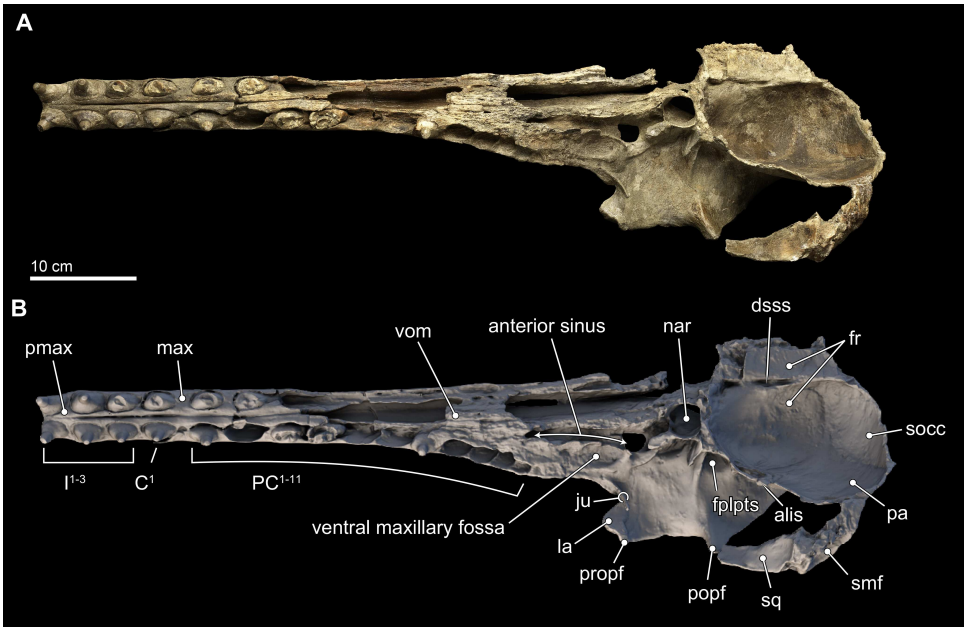

Figure 4 Skull in ventral view. Ventral views of the type skull of *Isthminia panamensis* (USNM 546125) from (A) photographs and (B) orthogonal digital three-dimensional polygon model prepared from CT data, with lighting and color modifications using the Smithsonian X 3D browser. See http://3d.si.edu/explorer?s=iEpExr to measure, modify, or download this model.

or other diagenetic factors, which displace the elements approximately 1–2 mm from their life positions. Most of the upper dentition is missing from the skull, except for the anterior teeth, some of which are complete; other more posterior teeth are incomplete, while three isolated teeth were recovered from the quarry at the type locality. Despite the heavy erosion that removed most of the left portion of this skull, sufficient anatomical details are preserved on the right side of the cranium, and along the rostrum to provide insights into the morphology of *Isthminia*.

Premaxilla. In dorsal view, the premaxilla dominates the visible part of the rostrum, comprising the entirety of the rostrum from its anterior end to about 75% of the length of the rostrum. In this view, the premaxilla occupies a width greater than that of the maxilla until the level of the maxillary flange (*sensu Mead & Fordyce, 2009*:62), where the width of the premaxilla begins to taper relative to the expansion of the maxilla overlying the cranium, in dorsal view (Fig. 3). Along the rostrum, anterior of the premaxilla-maxilla suture, there are several shallow longitudinal canals that terminate in small oval foramina (~5 mm long by ~2 mm wide). These canals are similar to those observed in adult specimens of *Inia*, but markedly different from the singular, deep groove that separates the posterior connection of the premaxilla and maxilla in *Pontoporia, Ischyrorhynchus*, immature specimens of *Inia*, and *Lipotes*. In *Isthminia*, adult *Inia* and *Lipotes*, these canals disappear posteriorly, as the premaxilla-maxilla suture becomes seamless along the length of the rostrum (Figs. 3 and 5).

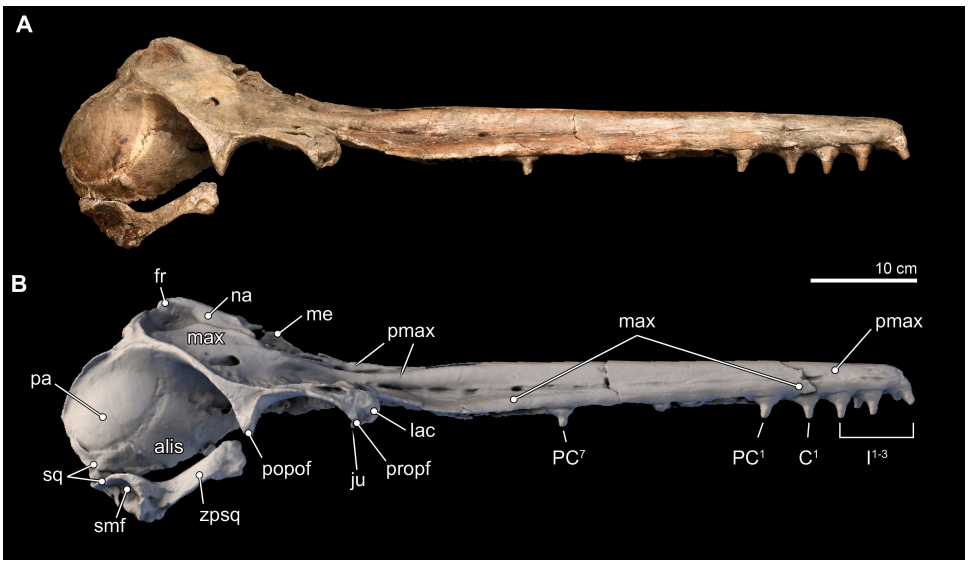

Figure 5 Skull in lateral view. Right lateral views of the type skull of *Isthminia panamensis* (USNM 546125) from (A) photographs and (B) orthogonal digital three-dimensional polygon model prepared from CT data, with lighting and color modifications using the Smithsonian X 3D browser. See http://3d.si.edu/explorer?s=jn4ynp to measure, modify, or download this model.

The paired right and left premaxillae are unfused for 4 cm at their anterior tip (Figs. 3A, 3B and 3D), presenting a slight gap, which is likely homologous in other odontocete taxa with the mesorostral groove (*sensu Mead & Fordyce, 2009*:16). This gap is then obscured posteriorly by full sutural fusion between the premaxillae for 24 cm along the midline of the rostrum until an elongate (6.9 cm-long) window is exposed between the overarching right and left premaxillae, just anterior of the level of the antorbital notches (Figs. 3A and 3B). Near the anterior origin of this window, the anteromedial sulcus appears, approximately at the transverse level of the last upper tooth alveolus (Fig. 4). This latter sulcus extends subparallel to the latter window until it terminates posteriorly in the premaxillary foramen. In *Inia*, the anteromedial sulcus extends farther anteriorly, and the portion of the premaxilla medial to the sulcus is more bulbous, while in *Pontoporia* the anteromedial sulcus is deeper, and nearly enclosed dorsally by overhanging flanges of the premaxilla. Fossil pontoporiids are broadly similar to *Pontoporia*, whereas in *Pan-Inia*, such as *Ischyrorhynchus* and *Meherrinia*, this area is not well preserved. At the level of the premaxillary foramen, the right and left premaxillae diverge from their midline fusion in separate paths around the external bony naris (Fig. 6). This divergence produces a V-shaped gap, 32 mm in anteroposterior length and 9 mm in lateral width, which is narrowed and longer than fossil pontoporiids, such as *Auroracetus*; this gap is small and variable in *Inia*, and broad and triangular in *Ischyrorhynchus* and *Meherrinia*.

The premaxillary foramen itself is thinly ovate, 11 mm anteroposterior length, and 4 mm wide (Fig. 6), unlike the small, subcircular foramina in other fossil inioids. (The left side of the cranium, from this level posteriorly is not preserved, and thus the remainder of the description necessarily uses the right side of the cranium). The posterolateral sulcus is

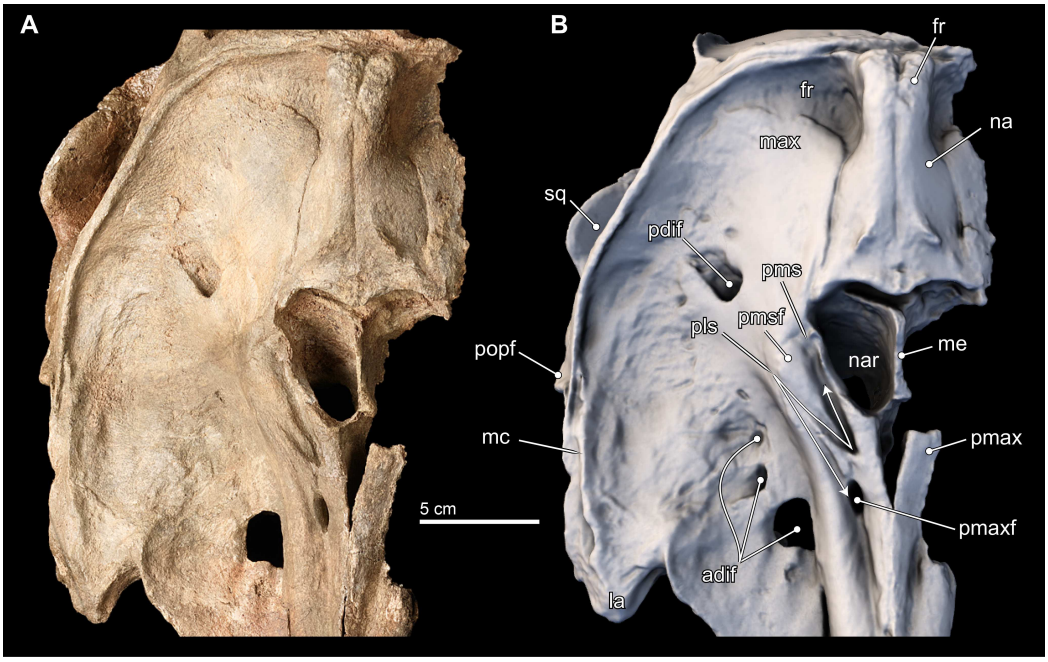

Figure 6 Close-up on vertex of skull. Close-up views of the vertex in the type skull of *Isthminia panamensis* (USNM 546125) from (A) photographs and (B) orthogonal digital three-dimensional polygon model prepared from CT data, with lighting and color modifications using the Smithsonian X 3D browser. See http://3d.si.edu/explorer?s=cGDc1L to measure, modify, or download this model.

shallow, and extends slightly laterally from its deepest portion at its origin, the premaxillary foramen. The posterolateral sulcus terminates posteriorly in a faint way at the level of the anterior margin of the external naris. This condition is similar to *Meherrinia* and *Brachydelphis*, while it is different from *Pontoporia, Auroracetus, Pliopontos*, *Pontistes* and *Inia*, which present a deeply excavated sulcus along the posterolateral edge of the premaxilla. This portion of the premaxilla is not well preserved in *Ischyrorhynchus*. Medially, the posteromedial sulcus is unusual in originating 9 mm posterior of the premaxillary foramen and bifurcating into lateral and medial tracts that delineate the borders of the premaxillary sac fossa. Along with the posterolateral sulcus, these bifurcating tracts create a Z-shaped sulci pattern that is shallow laterally and deep (>3 mm) anteromedially (Fig. 6B). The path of medial tract of the posteromedial sulcus extends along the lateral margin of the anterior half of the external naris, but it is not confluent with the border of the naris. This morphology is completely new, and not observed in any inioid nor delphinidan. The bifurcating tracts enclose a low, but convex premaxillary sac fossa located lateral to the external naris and dipping medially, whereas the premaxillary sac fossa in all other inioids is located anterolateral of the external naris and is strongly convex, except for *Meherrinia* and *Pliopontos*. This portion is not preserved in *Ischyrorhynchus.* The premaxillary sac fossa in *Lipotes* is flat, with elevated margins.

The patent posterior termination of the entire premaxilla is spatulate, flat, and it appears at the level of the posterior half of the external bony naris, as in *Meherrinia*. There is an 8 mm separation between the posteomedial termination of the premaxilla

and the anterolateral-most point of the nasal. In contrast, the posterior termination of the premaxillae of *Pontoporia* reaches the level of the posterior edge of the external nares, while in adult *Brachydelphis* spp., *Pliopontos*, *Pontistes*, *Inia*, and *Lipotes*, it extends even farther posteriorly; in young specimens of *Brachydelphis* and *Pontoporia*, it is in an intermediate position. Although there is slight erosion of the bony surface along the immediate margin of the external naris, the gap between the premaxilla and nasal is patent.

Maxilla. Throughout most of the anterior two thirds of the rostrum, the maxillae and premaxillae have a cylindrical outline (Fig. 3). Dorsally, the maxilla is exposed slightly on the lateral margin of the rostrum that is otherwise dominated by the premaxilla until about the proximal third of the rostrum where the maxilla becomes flatter along the maxillary flange. (As with the premaxilla, nearly all of the facial portion of the left maxilla has been lost to erosion, and the description is based on the right side). The antorbital notch is widely open, U-shaped, and oriented anteriorly. Posterior to the antorbital notch, the maxilla is expanded to cover most of the supraorbital process of the frontal, with the exception of the posterior-most and posteromedial edge, where the frontal is exposed. This posteromedial exposure of the frontal is similar to the condition observed in *Ischyrorhynchus* and *Inia* (mainly in juveniles), and differs from *Pontoporia, Pontistes, Pliopontos, Meherrinia, Brachydelphis* spp., and *Lipotes*, where the maxillae reaches the nuchal crest, and the lateral edges of the vertex. Posterolateral to the antorbital notch, the maxilla form a low maxillary crest (*sensu Mead & Fordyce, 2009*:51), which extends from the preorbital process, continues along the length of the supraorbital process of the frontal, but terminates at the postorbital process, unlike in *Inia*, where the crest continues well posterior of the postorbital process and join the temporal crest. In *Isthminia*, the maxillary crest is mediolaterally thicker (2–6 mm), but lower (∼5 mm), than the thinner, but higher (>5 mm) crest observed in *Inia*; in *Pontoporia* and *Pliopontos* this crest extends only the length of the supraorbital process.

Dorsally, the right maxilla shows a large diameter (∼10 mm) anterior dorsal infraorbital foramen, located at the level of the antorbital notch (Figs. 3A, 3B, 3D and 6). A second, anterior dorsal infraorbital foramen is posterolateral to the first one, and it is smaller in diameter (∼7 mm), and oriented posterolaterally. A single, posterior dorsal infraorbital foramen is located posterolateral to the external nares, it has a diameter of about 9 mm and its orientation is posterodorsal. The posterior dorsal infraorbital foramen of *Isthminia* is absolutely larger and located farther posteriorly than the corresponding foramen in *Inia, Ischyrorhynchus, Meherrinia, Brachydelphis, Pontistes, Pliopontos, Pontoporia*, and *Lipotes*.

In ventral view, the rostral portion of the maxilla bears alveoli for at least 14 maxillary teeth, with thin interalveolar septa (Fig. 4). At the ventral midline contact between the maxillae, there is a longitudinal groove that extends from anteriorly to about the level of the fifth maxillary tooth; a similar sulcus is also observed in *Inia* and *Pontoporia*, whereas this groove reveals a palatal exposure of premaxilla and/or vomer in *Ischyrorhynchus* and *Brachydelphis mazeasi*. Along the ventral surface and anteromedial to the jugal, there is a shallow (∼2 mm) oval (∼17 mm long by 10 mm wide) fossa; a similar fossa is also present in some specimens of *Inia*, *Ischyrorhynchus*, *Brachydelphis* spp. and very slightly

Pontoporia. Medial to this shallow fossa, which we term the ventral maxillary fossa, there is an elongated fossa that continues anteriorly parasagittally for about 60 mm, and 5 mm in width and depth. The location and morphology of this latter fossa corresponds to the anterior sinus of *Inia* (*Fraser & Purves, 1960*), and it is exposed in *Isthminia* because its overlying maxilla and palatine were eroded. An anterior sinus is also found in *Ischyrorynchus*, however it is shorter than that in *Inia* and *Isthminia*. The rostral portion is not preserved in the other genera of inioids, preventing any comparison.

Lacrimal and Jugal. The lacrimal appears to be ankylosed with the anterior margin on the supraorbital process of the frontal, forming its anterior surface, a condition common to all adult inioid specimens (Figs. 3–5). Ventrally, the lacrimal extends medially to join the jugal, which together forms the anteroventral surface of the antorbital notch. The preserved part of the jugal is a thin strut that is subcylindrical in outline (~4 mm wide; 17 mm long; ~2 mm thick) and oriented posteroventrally. Overall, it is very similar in morphology to the jugal of *Inia*.

Frontal. Dorsally, the frontal is mostly covered by the maxilla, but it is exposed along the posterior and posteromedial edges of the skull roof (Figs. 3 and 5–7). In *Isthminia*, the right and left frontals form the highest part of the vertex, and together form a pair of rounded, rectangular knobs with a slight midline cleft (Figs. 3A–3C, 5 and 6). This topographic high for the frontals at the vertex is similar in *Inia, Ischyrorhynchus* or *Meherrinia*, and even *Pontoporia* and *Lipotes*, although the frontals in *Isthminia* are small and low by comparison with *Pan-Inia*. Unlike *Inia* and *Meherrinia*, the midline cleft between the right and the left frontals at the vertex does not show participation of an anterior supraoccipital (or possibly interparietal) wedge externally nor in internal CT scan data (Fig. 7 and Video S1). The dorsal surface of the vertex is lightly rugose, but not as strongly as in adult specimens of *Inia*.

The supraorbital process is dorsoventrally thin (~5 mm) with a blunt preorbital process; in contrast, the postorbital process is more elongated with a triangular cross section through its longitudinal axis, similar to the general condition of the other inioids. Nevertheless the distance between this two processes (52 mm), reflecting the size of the orbit, is about twice that of adult specimens of *Inia*, but in *Isthminia* it is proportionally similar to the other fossil inioids (all known specimens of *Ischyrorhynchus* lack this feature; see Table 3). In dorsal view, the lateral edge of the supraorbital process is relatively straight and oriented parasagitally, unlike *Inia* and *Pontoporia* where this border is laterally concave and oriented anterolaterally, or the nearly straight but anterolaterally oriented borders of *Pliopontos* and *Brachydelphis*. Additionally, the postorbital process is shorter than the length of the orbit, contrasting with the much longer process and smaller orbit in *Inia*. The ventral surface of the supraorbital processes is gently concave with a low, but distinct postorbital ridge. Medially and posterior to the frontal groove there is a shallow (<1 cm) round (~1.5 cm diameter) fossa for the postorbital lobe of the pterygoid sinus. This same fossa varies tremendously in adult specimens of *Inia*, where it can either be shallow and slit-like (e.g., USNM 49582) or form a deep pit (e.g., USNM 239667). By contrast, this fossa in *Pontoporia* is deep, rounded and floored posteroventrally by the alisphenoid; in *Brachydelphis* spp., this fossa is shallow, as it is in *Lipotes*.

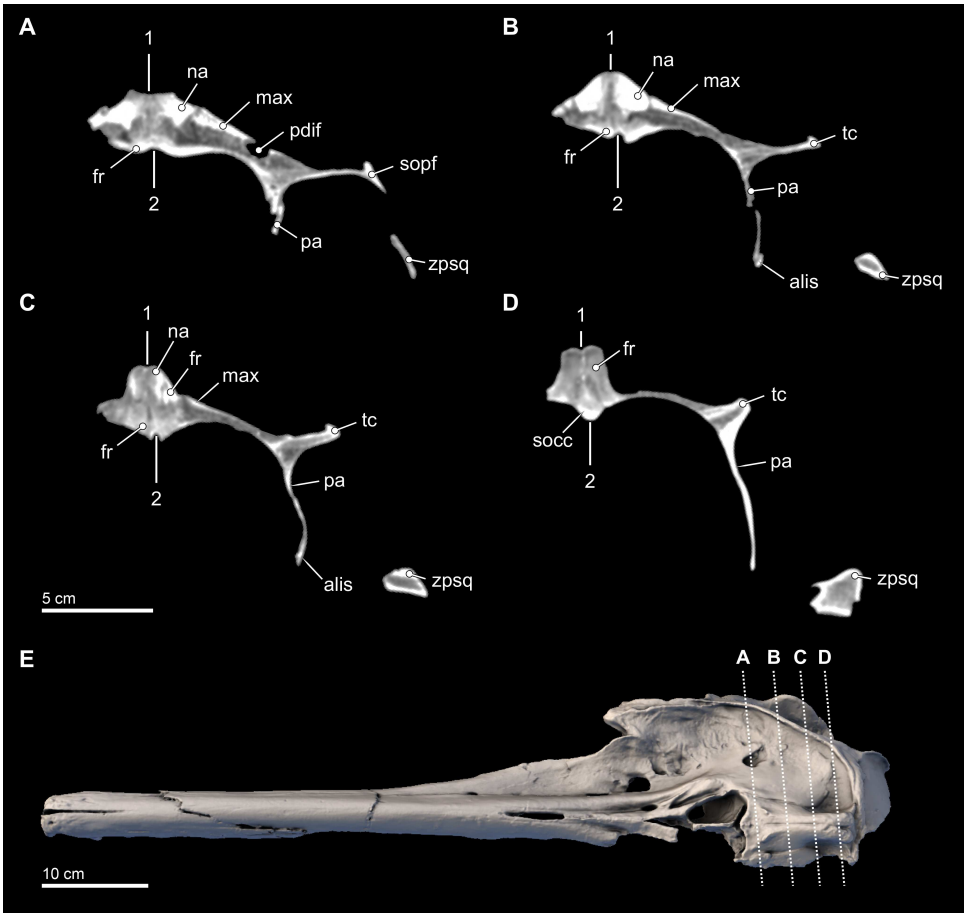

Figure 7 Transverse CT slices through the skull. Computed tomography (CT) slices through the vertex of *Isthminia panamensis* (USNM 546125) across four slightly sub-transverse planes that pass anterior to posterior (A–D). CT slices (A–D) represent respective CT slices numbers 20566, 20625, 20655, and 20708, available for download on the Smithsonian X 3D browser (http://3d.si.edu). Numbers 1 and 2 denote facial and endocranial sagittal midlines, respectively, showing the sinistral displacement of the facial bones typical in many odontocetes (*Geisler & Sanders, 2003*; *Mead & Fordyce, 2009*).

In the ventral view of the endocranium (Fig. 4), the right and left frontals surround the anterior aspect of the endocranium, where the extensive cerebellar juga are preserved on the ventral surface (*Mead & Fordyce, 2009*:18). Medially, the posteromedial margins of the frontals inside the endocranial region enclose a deep dorsal sagittal sinus sulcus along the midline. Such a structure is not visible in intact, extant skulls of *Inia* and *Pontoporia*, available for observation, nor is it preserved in most fossil inioids. Incomplete crania of *Brachydelphis* referable to *B. jahuayensis* (*Gutstein et al., 2009*: Fig. 7B) show no such sinus, but instead a low, bony ridge. Finally, a small wedge of the supraoccipital directly ventral to the vertex separates the fan-like posterior-most margins of the right and left frontals, which eventually contact the anterodorsal margins of the parietals along the frontoparietal sutures.

Nasal. The right and left nasals are paired at the vertex, sloping away from the topographic high of the paired frontals (Figs. 3, 5 and 6). Overall, the nasal is large (width = ~12 mm; length = 41 mm), dominating the anterodorsal surface of the vertex, and occupying the entire posterodorsal margin of the external bony naris. The anterior margin of nasal is concave. Together, the right and left nasals are anteroposteriorly elongate with some tapering posteriorly, as in *Pontoporia*, *Brachydelphis*, *Pontistes*, *Auroracetus*, *Pliopontos*. However, the nasal in *Isthminia* is dorsoventrally more massive than these latter genera, and it is not as anterodorsally inclined as in *Meherrinia* not as anterior-facing as in *Ischyrorhynchus*, *Inia*, and *Lipotes*.

The anterior margin of the nasal displays a low sigmoidal crest that extends transversely with a small protuberance that rises in the middle of the nasal, about 10 mm from its anterior margin; with the paired right and left nasals, these small crests and the base of these protuberances outline a wide, but shallow V-shaped concavity, pointing posteriorly (Figs. 3A, 3B and 3D). The posterior margin of the nasal is difficult to resolve without close inspection because the sutural distinction between the nasal and the frontal in this part of the vertex is overlapping and thin (see also Fig. 6). The posterior termination of the nasal overlaps with the frontal by passing in a broadly posteromedial path, terminating anterior of the level of the posteriormost margin of the maxilla. Together, the posterior termination of the right and left nasals show an anteriorly-pointed V-shaped margin. This condition is similar to *Pontoporia* and *Brachydelphis*, where the contact between the nasal and frontal shows a similar V-shaped margin; in *Auroracetus* and *Meherrinia*, a small wedge of the frontals insert medially between the nasals.

Vomer and Ethmoid. The vomer is poorly preserved ventrally, but a small portion is patent along the midline palatal surface adjacent to the medial margin of the highly eroded right maxilla, approximately extending 45 mm, with an anterior extent to the transverse level of the 8th maxillary tooth alveolus (Fig. 4). The ethmoid is incompletely preserved; the crista galli is shallow with very small (<1 mm) foramina in its surface. The ethmoid forms the bony nasal septum, rising dorsally to the same horizontal level as the premaxillae, but not quite reaching the level of the nasals. The lateral wings form the posterior and posterolateral walls of the external nares, which are cleanly separated from the anterior margin of the nasals by a continuous gap 5–8 mm wide (Fig. 6).

Parietal. The parietal is exposed broadly on the posterior margin of the temporal fossa, along with the frontal and squamosal (Figs. 3C, 3D, 5 and 7). The lateral surface of the parietal is smooth and convex; in posterior view, the temporal crest of the parietal is posterolaterally oriented, as opposed to the ventrally oriented crests in *Inia* and *Pontoporia*. The anterior extent of the parietal is unclear because the parieto-frontal suture is not patent, similar to adult specimens of *Inia*.

Supraoccipital. Only the dorsal half of the supraoccipital can be reliably determined for *Isthminia*. Dorsally, the supraoccipital does not participate in the vertex, but participates in the temporal and nuchal crests (Figs. 3A–3C); the nuchal crest is transversely straight, about 10 mm thick, and unlike the more anteromedially oriented crest in *Inia* and the posteriorly concave crest of *Pontoporia*. Posteriorly, there is a midline external occipital

crest that is bounded laterally by deep (9 mm) semilunar fossae; such fossae are also patent in adult specimens of *Inia* and *Pontoporia*. The external surface is smooth and convex. The temporal crests are nearly vertical, and dorsally they join the nuchal and orbitotemporal crests (*sensu* *Fordyce, 2002*:194), forming a tabular, triangular surface at the triple junction. When viewed posteriorly, the supraoccipital has a square outline, unlike the more sub-triangular outline in *Inia*, or the general pentagonal outlines of *Pontoporia* and *Lipotes*.

Squamosal. The right squamosal is nearly completely preserved. The zygomatic process of the squamosal is relatively long, mediolaterally thin, laterally convex, and medially concave. Overall, its main corpus is rectilineal in lateral view, in contrast to the gently tapering profile of *Pontoporia* and acute tapering in *Inia*. In *Isthminia*, the anterior tip of the zygomatic process is expanded, with a squared-off anterior margin, more like *Inia*, and to a lesser degree *Brachydelphis mazeasi*, rather than the rounded, tapering tip of *Pontoporia and Pliopontos*. The dorsal surface of the root of the zygomatic process in *Isthminia* is concave, while its lateral edge flares outward about 10 mm farther laterally than the anterior part of the process (Figs. 3–5). In lateral and ventrolateral views, the postglenoid process is not patent, but it shows no indication of supporting elaboration, such as the bulbous postglenoid process in both *Inia* and *Pontoporia*, and acute and thin in *Brachydelphis* spp. (*Gutstein et al., 2009*; *Lambert & de Muizon, 2013*). Ventrally, the outline of the glenoid fossa in *Isthminia* is elongate, shallowly convex, and faces ventromedially. The tympanosquamosal recess extends as a deep (∼5 mm) sulcus medial to the glenoid fossa, as it does in other inioids. The posterolateral surface of the squamosal has a broad and relatively deep concave sternomastoid fossa, deeper than *Inia*.

The squamosal plate is relatively low, occupying only about the lower quarter of the surface of the temporal fossa, which is dominated by the parietal (Fig. 5). This configuration is similar to the condition seen in *Pontoporia* and *Brachydelphis*, but contrasts with *Inia*, where the squamous portion is much higher, a condition also visible in *Lipotes*. The anterior extent of the squamosal plate is ankylosed with the posteroventral edge of the temporal wall exposure of the alisphenoid in the type specimen of *Isthminia*.

Alisphenoid. Only the dorsal portion of the alisphenoid is preserved in the type specimen of *Isthminia* above the horizontal level the squamosal fossa (Fig. 5). In lateral view, the parieto-alisphenoid suture extends in a path from the squamosal plate at the posterior margin of the temporal fossa dorsally to a level in line with the nuchal crests; in this way, this sigmoidal suture partitions the parietal (dorsally) and the alisphenoid (ventrally) in the middle of the temporal fossa. The anterior margin of the alisphenoid extends at least to the level of the postorbital processes of the frontal, although the actual sutures are not patent at the anterior end (see also Fig. 7). In lateral view, the dorsal extent of the alisphenoid on the temporal wall is much greater than that seen in *Inia*, but we note a degree of variability in *Inia*.

Mandible

Both right and left mandibles are preserved intact and remain articulated via an osseous symphyseal articulation (Figs. 8 and 9; Class IV jaw joint of *Scapino, 1981*). The length

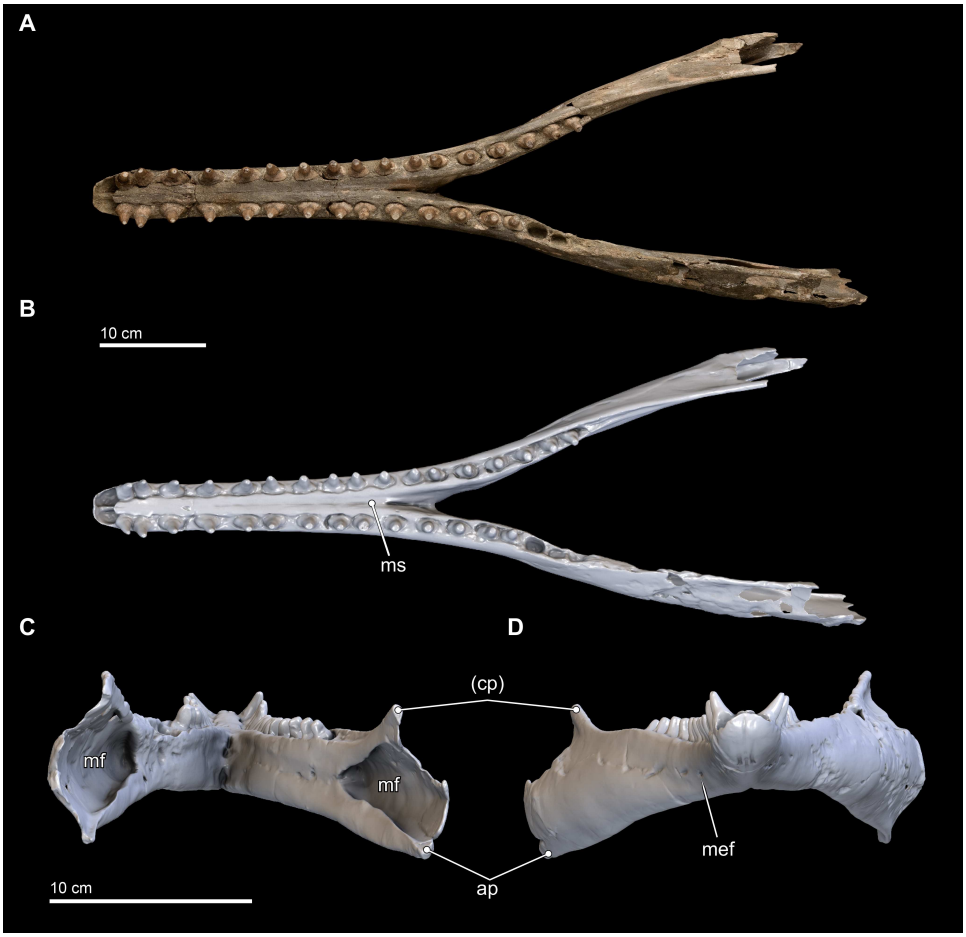

Figure 8 Mandibles in dorsal, anterior, and posterior views. Dorsal views of the mandibles of *Isthminia panamensis* (USNM 546125) from (A) photographs and (B) orthogonal digital three-dimensional polygon model prepared from CT data, with lighting and color modifications using the Smithsonian X 3D browser. (C) Anterior and (D) posterior views of the mandibles of *Isthminia panamensis* (USNM 546125) from orthogonal digital three-dimensional polygon model prepared from CT data. See http://3d.si.edu/explorer?s=hhl3iu (dorsal view), http://3d.si.edu/explorer?s=cgvhM3 (posterior view), and http://3d.si.edu/explorer?s=gR4Rhv (anterior view) to measure, modify, or download this model. Parentheses denote missing structure(s).

of the mandibular symphysis (21.0 cm) is approximately 43% of the entire length of the mandible. The mandibles possess nearly all of the original lower teeth; the lower first incisors are missing, along with posterior most three teeth of the right mandible (although one isolated tooth is a perfect fit for PC_{12}; see Fig. 10). Both the right and left mandibles possessed 18 and 17 lower teeth, respectively, although the degree of bone remodeling posterior of left PC_{13} leads us to presume that 18 teeth is the likely maximum lower tooth count (Fig. 10). Posterior margins are incomplete for both sides of the mandible, and the left angular process appears intact and there is a weak suggestion of the osteological structure where the left articular condyle would have been. The right articular condyle is missing. Most of the mandibles are well preserved, although much of the right acoustic window is degraded from erosion and/or diagenesis (Fig. 9).

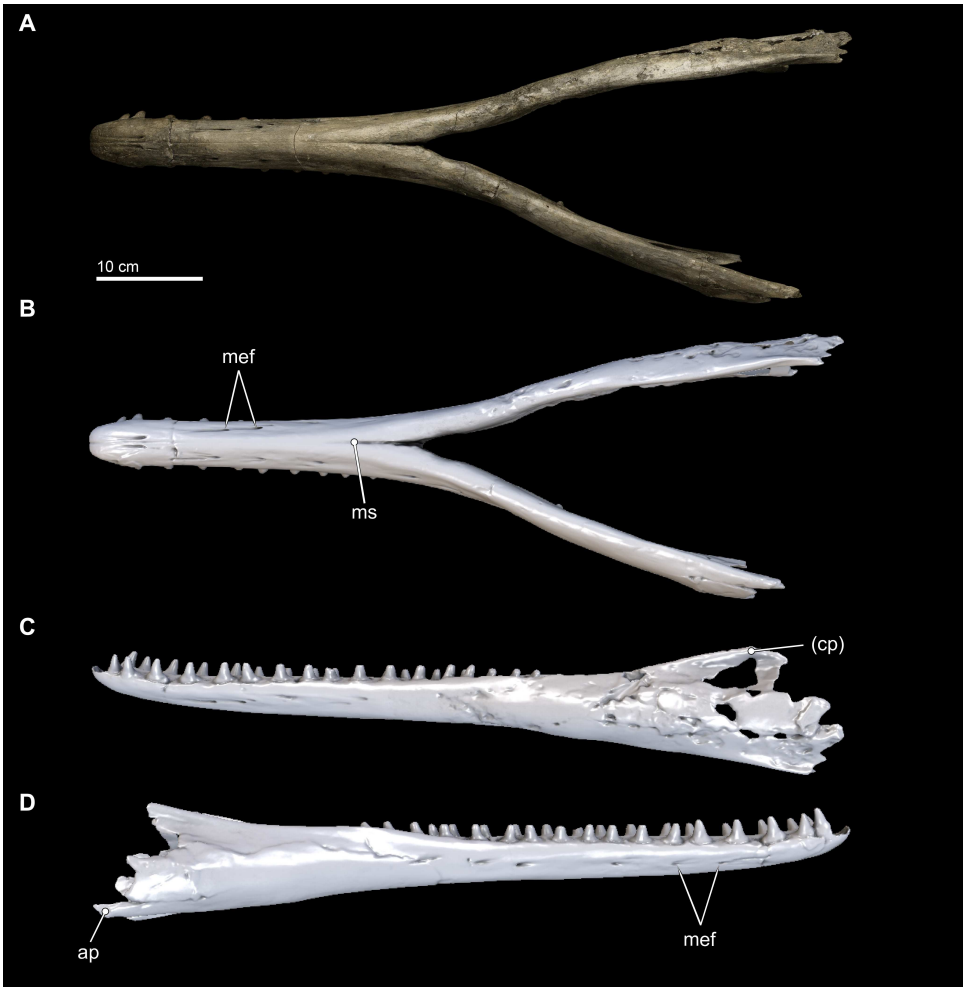

Figure 9 Mandibles in ventral and lateral views. Ventral views of the mandibles of *Isthminia panamensis* (USNM 546125) from (A) photographs and (B) orthogonal digital three-dimensional polygon model prepared from CT data, with lighting and color modifications using the Smithsonian X 3D browser. (C) Left lateral and (D) right lateral views of the mandibles of *Isthminia panamensis* (USNM 546125) from orthogonal digital three-dimensional polygon model prepared from CT data. See http://3d.si.edu/explorer?s=cavfn3 (ventral view), http://3d.si.edu/explorer?s=dGTRVj (left lateral), and http://3d.si.edu/explorer?s=cLO5aZ (right lateral) to measure, modify, or download this model. Parentheses denote missing structure(s).

In anterior view and posterior views (Figs. 8C and 8D), the mandibles show slight asymmetry in the relative directions of the overall mandibular rami, with the right ramus extending laterally and slightly ventral relative to the left one. This asymmetry may be diagenetic and related to sediment compaction, but we think it more likely records the original right-left asymmetry that is common in other living inioids (*Werth, 2006*), and this condition is evident in adult specimens of *Pontoporia*, with its proportionally elongate rostrum. In ventral view, the anterior termination of the mandibles from the gnathion to pognion is gradual and not acute, with a ventral outline that is somewhat rectangular. Anteriorly, this termination is flat and not acute. Posteriorly, the ventral surface of the

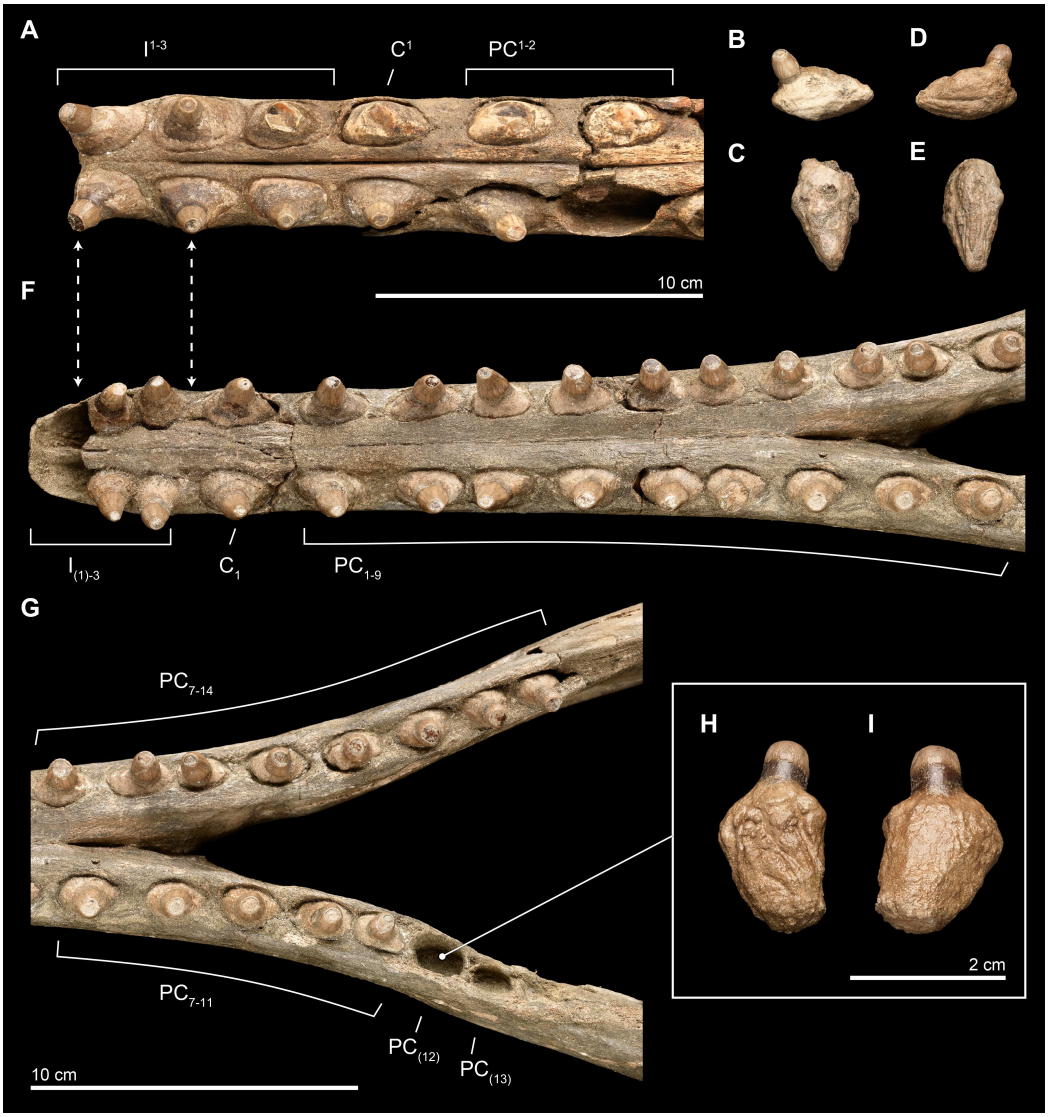

Figure 10 Close-up of upper and lower dentition. The dentition of *Isthminia panamensis* (USNM 546125) in close view. (A–E) Upper dentition including the rostrum (A) and isolated teeth collected near the skull at the outcrop surface, showing (B), an upper left posterior tooth (likely PC^3) and (C), an upper left posterior tooth. (F–I) Lower dentition including the mandible (F, G), shown in two parts, with overlapping images over the mandibular symphysis. (H–I) An additional isolated left tooth posterior (almost certainly PC_{12}) was collected at the type locality. Dashed lines with arrowheads indicate alignment for the occlusion of upper and lower dentition.

mandibles is U-shaped, in transverse section, through the symphysis. Generally, this morphology is most similar to that of *Inia*, and *Saurocetes argentinus* Burmeister, 1871, which is only known from a mandibular fragment that is less complete than *Isthminia* (Cozzuol, 1989; Cozzuol, 2010). The general lateral and horizontal profiles of the mandible in *Isthminia* are unlike *Pontoporia*, with a deep lateral groove, and unlike the strongly convex mandibles of *Brachydelphis mazeasi* (based on MUSM 887).

The ventral margins of the mandible, posterior of the symphysis, are rounded until the posterior half of the level of the acoustic window when this margin gradually gains an edge (Fig. 8D). The medial profile of the acoustic window in *Isthminia* is dorsoventrally narrower than that of *Inia*, and considerably more acute than *Pontoporia*. Both right and left mandibles show approximately 7 mental foramina each, spaced along the ventrolateral margins of the mandibles along the symphysis. In each case, the foramina open anteriorly, often forming sulci with long tails. The anterior most foramina are paired close to the midline of the symphysis at the level in between the third and fourth lower tooth. *Isthminia* shares a high number of mental foramina with *Inia*, whereas both *Pontoporia* and *Brachydelphis mazeasi* shows fewer (1–2 mental foramina in adult specimens of *Pontoporia*, and 4 mental foramina in MUSM 887).

The overall morphology of the mandibles in *Isthminia* shares the most similarities with *Inia*, among inioids and delphindans for which this element is known, especially in lateral and horizontal profiles anterior to the symphysis. Posterior of the symphysis, the rami of the mandibles are lower than *Inia*, and slightly more gracile. The mandibles of *Isthminia* are also not dorsoventrally flattened like those of *Pomatodelphis inequalis* *Allen, 1921*, nor are they slender like those of *Kentriodon pernix* *Kellogg, 1927* (USNM 8060) and *Brachydelphis mazeasi* (based on MUSM 887). The mandibles of *Isthminia* differ strongly from *Lipotes*, and fossil delphindans such as *Lophocetus pappus* *Kellogg, 1955* (USNM 15985) and *Hadrodelphis calvertense* *Kellogg, 1966* (USNM 23408, 189423), which all notably have many more teeth posterior of the symphysis, and exhibit rounded, nearly circular alveoli. Ovate alveoli are notable in putative inioids represented by fragmentary mandibles, such as *Saurocetes argentinus* and *Hesperocetus californicus* *True, 1912* (UCMP 1352), although the dentition of *Isthminia* is far less bulbous than either. In *Goniodelphis hudsoni*, another putative inioid, the mandibles are relatively deeper, and mediolaterally flattened, with a much longer symphysis, and mediolaterally flattened teeth that are triangular in outline when viewed laterally, and with crowns are much more slender and somewhat recurved (see below).

Dentition

Upper. The upper dentition consists of 15 teeth per side, counted by alveoli in the premaxilla and maxilla on the right side of the skull. It is less complete than the lower dentition. Of the original upper dentition, only a total of 14 teeth remain preserved in their alveoli, with 6 in the left side and 8 in the right. Of these intact teeth, the right side preserves only the 2 distalmost teeth with crowns, while the others only preserve the tooth roots, with fractures at the base of the crown that are probably postmortem. An isolated upper right tooth discovered during excavation fits well in the third postcanine (PC^3) alveolus, and the lack of any preserved alveoli posterior to this level increases the likelihood of this placement being correct, although there is no way to eliminate a more posterior placement (see Fig. 10). Another isolated tooth root lacking the crown likely belongs to a right alveolus in the posteriormost dentition that is not preserved on this side of the skull. The left side preserves intact teeth, with crowns, from the first incisor (I^1) to PC^1 and then

an open alveolus at PC^2, followed by two tooth roots with rounded breaks where crowns were likely present prior to death. Right PC^7 is intact, although all of the other alveoli on this side are missing their teeth.

Overall, the teeth have slightly anteroposteriorly expanded tooth roots, exhibiting an ovate outline in occlusal profile at the margin of the alveolus, which is very similar to *Goniodelphis*, *Hesperocetus* and *Ischyrorhynchus*, although *Isthminia* has more clearly ovate tooth alveoli than all of these. By comparison, *Inia* and *Lipotes* have subcircular tooth outlines at the alveolar margins, whereas *Pontoporia* show nearly rectangular outlines. The posterior roots of the upper teeth are somewhat gibbous, with closed pulp cavities distally. The exposed base of the tooth roots, ventral of the level of alveolar margin, tapers dramatically towards the base of the tooth crown, with the crown situated more or less centrally on the tooth root, except for the anteriormost pairs of incisors, which are slightly procumbent. The base of the upper tooth crowns range from 11–12 mm in diameter, with very light longitudinal striae that surround the perimeter of the base (such light striations are visible on both lower and upper teeth). The enamelocementum boundary between the roots and the crown is distinct and sharp for both upper and lower teeth. The apices of the upper tooth crowns are worn, leaving subcircular tooth wear outlines through the enamel into the dentin that is polished. With the exception of the first incisors, the crowns of the upper dentition exhibit a slight buccal curve. Wear facets can be noted on the posterior margins at the base of the tooth crown in the first incisors and on the anterior side of right PC^1.

Lower. The lower dentition is nearly complete, consisting at most of 18 teeth per side, and missing only the first lower incisors and the two posteriormost left postcanine teeth. The right side consists of 18 teeth, whereas the left side consists of 17 teeth, although there are signs of bone remodeling where the alveolus of PC_{14} may have been. An isolated lower left tooth found during discovery quarrying fits reasonably well in the left PC_{12} alveolus, and the morphology and wear on the tooth crown matches its intact right counterpart (see Fig. 10). Like the upper dentition, the lower teeth posterior of the incisors are broadly ovate in occlusal profile, formed by the margins of the alveoli.

The near complete lower dentition provides detailed information about the morphology of the tooth crowns throughout the mandible for which the upper dentition only provides limited information. While the lateral profile of the lower dentition shows that the teeth are generally oriented vertically, but viewed along the major axis of the mandible, the anterior teeth from the canine (C_1) to PC_3 show buccal curvatures with slight lateral compression and mesiodistal keels that grade into straighter teeth without mesiodistal keels posterior of PC_3 and that also have more apical tooth wear, leaving less of the original tooth crowns. Generally, lower dentition posterior of PC_3 are rounder in occlusal profile, with slight lingual protuberances on the crown beginning at PC_6 that become more patent as true lingual cusps posterior of PC_9. After this level, the lower teeth grade slowly to presenting a more lingual orientation. Posterior of the termination of the mandibular symphysis, the diastemata shorten between adjacent lower teeth, although there is still enough space between the posterior most teeth to permit interlocking occlusion with the

corresponding upper dentition. Most of the lower teeth lack non-occlusal wear facets, except for the right I_2 and left PC_9.

Careful manual articulation of the lower jaw with the rostrum using full size 3D prints of the type specimen shows that the lower and upper dentition interlock in a precise, alternating way similar to extant odontocetes (e.g., *Tursiops Gervais, 1855*) with robust dentition. Although both lower teeth and upper teeth have crown base diameters in the same range (11–12 mm in mesiodistal diameter), the slightly shorter lower dentition diastemata provides the space for upper and lower teeth to slide past one another. Unusually, $I_{2–3}$ together pass posterior and anterior of $I^{1–2}$, respectively, although such imprecise occlusions do occur in other odontocetes, and such a similar pairing in the dentition can be observed in *Inia* (the posterior lower teeth of USNM 49582).

Scapula

Only the right scapula is preserved in the type specimen of *Isthminia* (Fig. 11). In dorsoventral dimensions, the preserved element is 16.8 cm tall, and approximately 15 cm in anteroposterior length (Table 2). The scapula is incomplete, and the following parts are missing from the type specimen: most of the dorsal margin, and especially most of the anterior aspect; most of the acromion; and the anterior tip of the coracoid process. The posterior margin of the suprascapular border is intact, as well as the glenoid fossa and most of the region surrounding the ventral aspect of the scapula.

The scapula is broadly fan-shaped, although it is exceedingly thin along the broken dorsal border, ranging from 1–3 mm in mediolateral thickness (Fig. 11). Nearly the entire part of the scapula housing the supraspinous fossa is missing, and only the basal 2 cm of the spinous process at its L-junction with the base of the acromion is preserved. The infraspinous fossa is deep, and it is the most concave aspect of the scapular topography in lateral view. Consequently, in medial view, the costal surface of the scapula shows corresponding and marked convexity. The depression for the teres major muscle is shallow, but patent. In dorsal view, the most striking aspect of the scapular morphology is the sinusoidal profile of the dorsal border created by the deep infraspinous fossa.

The acromion is incomplete, but the preserved base shows that it was dorsoventrally tall (25 mm) relative to the same dimension of the coracoid process, thin (4 mm in mediolateral thickness), and curved medially from its base; reminiscent of the condition observed in *Inia*. This morphology differs from the anteriorly rounded, subtriangular outline of the acromion of *Brachydelphis mazeasi* (MUSM 887) and *Pontoporia*, where the proximal end of the acromion is dorsoventrally broad and tapers distally. In lateral view, the angle formed by the acromion and the spinous process in *Isthminia* is nearly 90°, and the anterior margin of the scapular border bisects this angle at about 70°from the dorsal margin of the acromion. The coracoid is stepped medially from the level of the acromion, and it is thicker laterally than the acromion, with a slight lateral curve, and presents a slightly spatulate anterior termination, which is typical in delphinidans.

The glenoid fossa is 13 mm deep at its deepest, relative to its ventral margins. In ventral view, the overall shape of the glenoid fossa is roughly that of a slightly laterally compressed

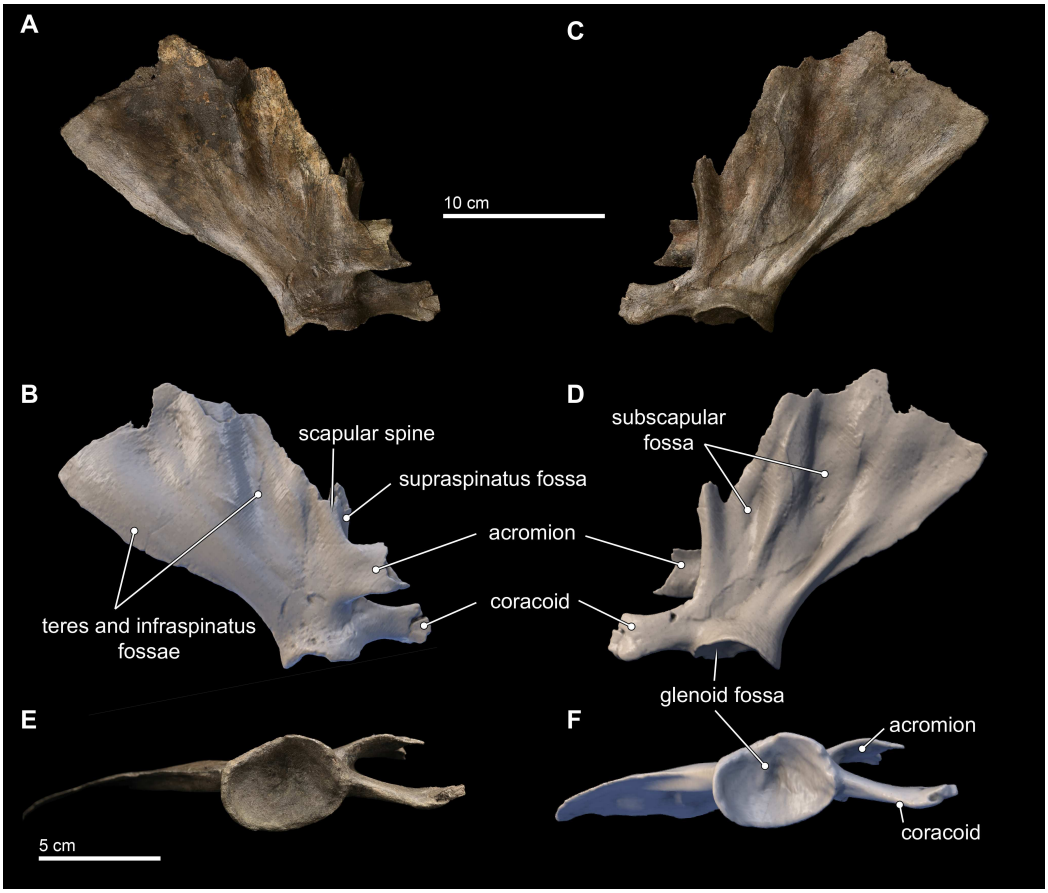

Figure 11 Scapula in lateral, medial, and distal views. Right scapula from *Isthminia panamensis* (USNM 546125) in lateral (A–B), medial (C–D), and distal (E–F) views. Each respective paired view shows photographs alongside orthogonal digital three-dimensional polygon model prepared from CT data, with lighting and color modifications using the Smithsonian X 3D browser. See http://3d.si.edu/explorer?s=dmsTMl (lateral view), http://3d.si.edu/explorer?s=jPwTGO (medial view), and http://3d.si.edu/explorer?s=hwGm9l (distal view). Anatomical terminology for the scapula follows *Tanaka & Fordyce (2015)* and *Uhen (2004)*.

oval (Figs. 11E–11F); when combined with its depth, the overall topography of the glenoid fossa is reminiscent of an ice cream scoop. A sharp posterior margin of the posterior scapular border extends to the margin of the glenoid fossa.

Carpals

Two carpal elements were collected in close proximity to the cranial elements of *Isthminia*, disarticulated and in isolation (Fig. 12). Both elements are mediolaterally flattened with anterior, posterior, proximal, and distal surfaces that are shallowly concave to convex, forming articular surfaces with the radius, ulna, other carpals, or metacarpals. Both carpal elements also have one surface that is well preserved, while another that is highly eroded. It is difficult to side isolated cetacean carpal elements; the only other preserved postcranial element is the right scapula, which provides one argument for considering these isolated

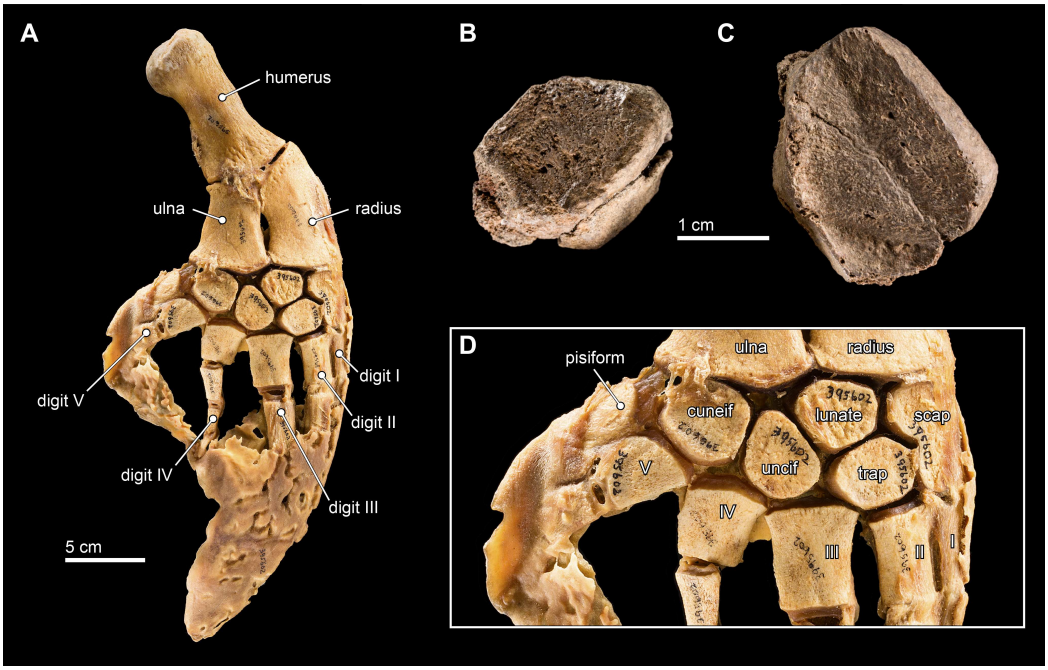

Figure 12 Carpal elements. (A) Complete, intact left pectoral limb of *Inia geoffrensis* (USNM 395602), showing all of the individual osteological elements in articulation. Carpal elements belonging to *Isthminia panamensis* (USNM 546125) include (B) a possible pisiform; and (C) a likely unciform, with (D) a close up of the carpal bones in (A), for comparison.

elements as belonging to the right side, although we cannot exclude the possibility that they each belong to different sides.

We compared these two isolated carpals with an articulated forelimb of *Inia geoffrensis* (USNM 395602, see Fig. 12) as well as with other odontocetes (*Cooper et al., 2007*). The smallest carpal element (Fig. 12B) represents either the cuneiform or the pisiform. It has a roughly lozenge outline, and it is about 50% smaller than the larger carpal element, which makes its identity as the pisiform more likely, given its association with the larger carpal. Interpreted as a pisiform, its anterior and distal surfaces are flat and likely articulated with the cuneiform and metacarpal V, respectively. A small pisiform is observed in *Inia*, as well as in other delphinoids (*Cooper et al., 2007*), while it seems to be lost in other, more distantly related river-inhabiting taxa (e.g., *Platanista gangetica*, USNM 172409). The larger carpal (Fig. 12C) has an irregular pentagonal outline, which limits its identity to the unciform, cuneiform, or lunate. The proximal facets of the unciform and cuneiform articulate with metacarpals IV and V, respectively. Given the length of the longest articular facet of this element, in direct comparison with the articulated forelimb of *Inia* (USNM 395602), we propose that this element most likely corresponds to the unciform.

Phylogenetic analysis

We obtained six most parsimonious trees (length = 1,922; ensemble consistency index = 0.283, and ensemble retention index = 0.451), in our phylogenetic analysis, with the strict consensus cladogram shown in Fig. 13. The resulting topology is overall very

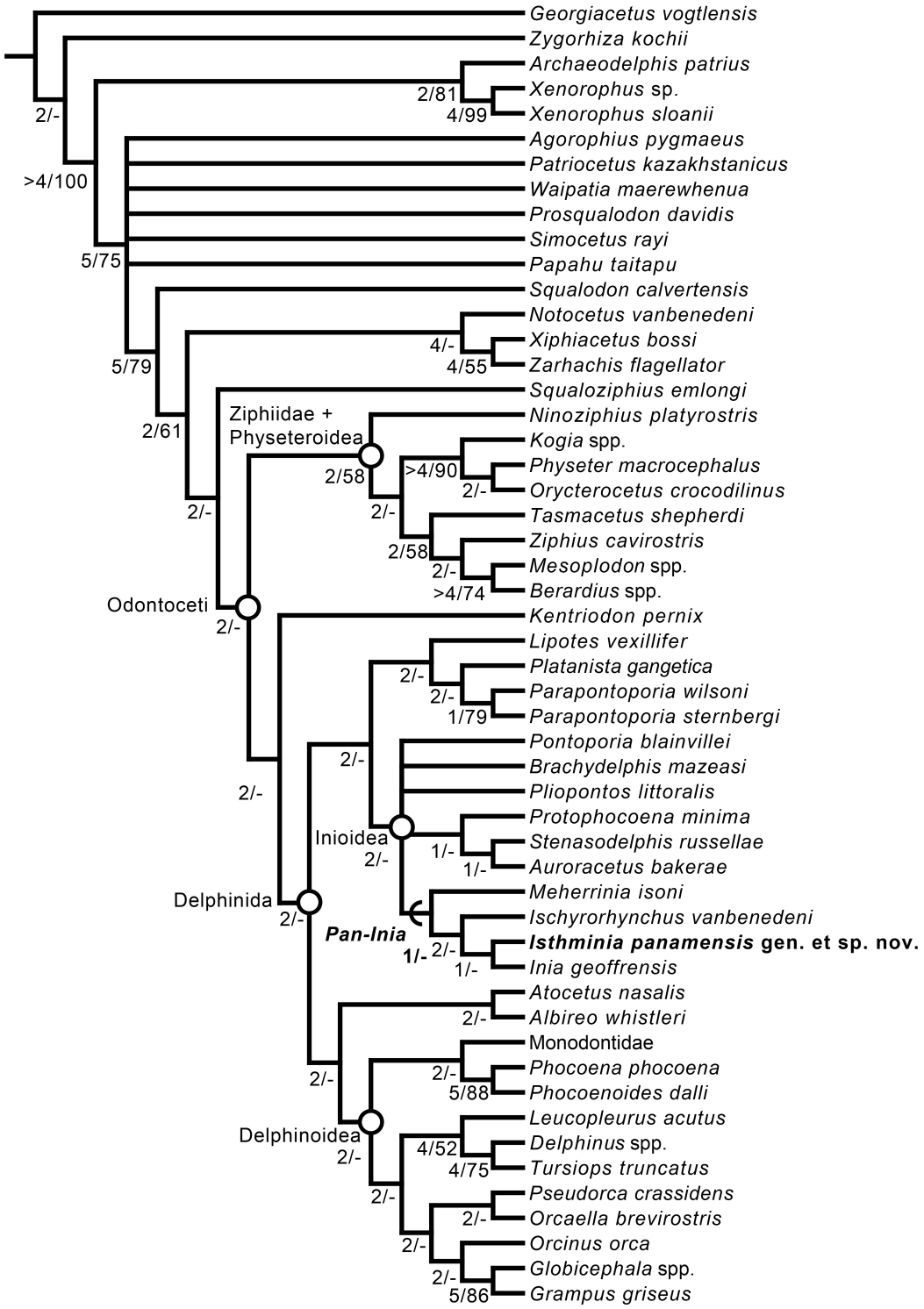

Figure 13 Strict consensus cladogram. Phylogenetic analysis of *Isthminia* and other inioid odontocetes, showing a strict consensus cladogram resulting from six most parsimonious trees, 95 steps long, with the ensemble consistency index equal to 0.283 and the ensemble retention index equal to 0.451. Numbers below nodes indicate decay index/bootstrap values; stem-based clades are indicated by arcs, while open circles denote node-based clades.

similar to that obtained by *Aguirre-Fernández & Fordyce (2014)* (see their Fig. 8), with the notable difference that the relationship of *Pontoporia*, *Brachydelphis* and *Pliopontos* with other inioids which is unresolved in our analysis, yielding a polytomy for Pontoporiidae (*sensu Geisler, Godfrey & Lambert, 2012*). Our results also resolved a clade (*Pan-Inia*) of taxa more related to *Inia* than *Pontoporia*, which consists of: *Meherrinia*, *Ischyrorhynchus* and *Isthminia*, the latter which is sister to *Inia*. Although Bremer support values for most of these nodes is low (i.e., 1 step), there is stronger support (i.e., 2 steps) for the clade that includes *Ischyrorhynchus* + *Isthminia* + *Inia*. The new position of *Ischyrorhynchus* is likely a result of our rescoring of several characters based on observations of the type and additional specimens of *Ischyrorhynchus*. This position differs from all previous phylogenetic analyses (e.g., *Geisler, Godfrey & Lambert, 2012*; *Aguirre-Fernández & Fordyce, 2014*) but it is consistent with *Cozzuol (2010)*'s proposal for a subfamily grouping of Ischyrorhynchinae within Iniidae (*Cozzuol, 1996*). Our analysis did not include *Saurocetes* spp., a large *Pan-Inia* known from the late Miocene age Ituzaingó Formation of Argentina and Solimões Formation of Brazil, and represented mainly by fragmentary mandibular remains (*Cozzuol, 1996*; *Cozzuol, 2010*). We also did not include *Goniodelphis hudsoni* from the Mio-Pliocene age Bone Valley Formation of Florida (*Allen, 1941*), which is represented by a poorly preserved cranium with some similarities to *Ischyrorhynchus*. Both taxa require reexamination that remains outside the scope of this study.

Our results differ in resolving a clade grouping *Lipotes*, *Platanista* and the fossil lipotid *Parapontoporia* spp., which shares some similarities with Platanistoidea *sensu Simpson (1945)* and *Geisler & Sanders (2003)*. The recovery of *Platanista* in a close relationship with other *Lipotes* has previously been recovered in the exclusively morphological analyses of *Geisler & Sanders (2003)* and *Aguirre-Fernández & Fordyce (2014)*, whereas exclusively molecular and combined molecular and morphological analyses consistently recover *Platanista* as a separate, basal branching clade from *Lipotes* and Inioidea, likely reflecting long branch attraction (see *Geisler et al., 2011*: Figs. 1 and 2, and references therein). Regardless, both morphological and molecular (and combined) analyses have consistently recovered Inioidea as a clade (i.e., *Inia* and *Pontoporia*), a finding replicated by our own results, herein.

DISCUSSION

Isthminia compared with other living and extinct inioids

Among inioids, the general morphology of *Isthminia* in dorsal view most resembles the known elements of *Meherrinia* and *Inia*, although the broad circular outline of the maxillae and their contact with the vertex is also reminscient of *Brachydelphis*. In ventral view, *Isthminia* is most similar to *Ischyrorhynchus* and *Goniodelphis*, although both of these taxa are represented by more fragmentary remains than *Isthminia*. The rostrum of *Isthminia* is robust, with dorsal fusion between the right and left premaxillae, and possessing relatively robust upper and lower dentition, with strong wear on the apical crowns, although *Isthminia* does not exhibit lingual cusps in the posterior dentition observed in *Inia*. Additionally, tooth counts are more similar to *Inia*, certainly more so than *Pontoporia*.

The strong groove separating the premaxilla and maxilla along the length of the rostrum is most similar to *Inia*, whereas *Pontoporia* and *Ischyrorhynchus* show a small but deep indentation that runs the length of the rostrum. In some ways, the rostrum of *Isthminia* is reminiscent of *Kampholophos serrulus* Rensberger, 1969 (UCMP 36045), from the late Miocene of California, which has dentition that is far more crenulated than *Isthminia*. In several basic traits (e.g., robust dentition reduced in number, robust rostrum, and a broad exposure of the temporal fossa), *Kampholophos* shares many similarities with *Pan-Inia*, although its phylogenetic position has not been determined beyond potential membership in Delphinida (see Salinas-Márquez et al., 2014).

Isthminia exhibits a large dorsal infraorbital foramen on the maxilla, which is proportionally similar to *Inia* and *Ischyrorhynchus*, although absolutely larger in *Isthminia* (Figs. 3 and 6). In ventral view, *Isthminia* shows anteriorly elongate anterior sinus system, invading the maxilla, a feature observed also in *Inia* (Fraser & Purves, 1960). Overall, the lateral profile of the rostrum in *Isthminia* remains in the same level as the cranium, whereas both *Pontoporia* and *Inia* shows a slightly dorsal elevation of its orbits, a featured most pronounced among odontocetes in *Lipotes*. Using the small crest on the supraoccipital as an external demarcation of the hemispherical midline of the underlying dermocranium, we note that the vertex in *Isthminia* is slightly sinistral (see also Fig. 7), to the same degree as *Inia*, and more so than *Pontoporia*, although not as highly sinistral as *Lipotes*. Interestingly, *Isthminia* lacks the strongly elevated and knob-like vertex of *Inia* and *Ischyrorhynchus*, maintaining a lower vertex profile similar to *Meherrinia*, *Brachydelphis*, and *Pontoporia*, although its frontals do form the absolute apex just as they do in *Inia*, with a pedestal that can be directly pinched between an index finger and thumb, anterior of the apex of the supraoccipital shield. Notably, *Isthminia* lacks the strongly inflated bosses of the premaxillary sac fossae seen in nearly all other inioids (Figs. 5 and 6).

The mandible of *Isthminia* is most similar to *Inia*, in terms of an elongate mandibular symphysis, morphology in transverse section, and general size (Figs. 8 and 9). Both *Isthminia* and *Inia* lack the distinct ventrolateral groove in *Pontoporia*. Mental foramina with overhanging sulci are prominent in *Isthminia*, but smaller in *Inia*, although in both they extend posteriorly along the body of the ramus; also, the anterior termination of the mandibles in *Isthminia* is rounded in lateral view, whereas it is more angular in *Inia*. In lateral view, the coronoid process in *Isthminia* is less elevated, relative to the level of the trough in the mandibular symphysis than either *Inia* or *Pontoporia*. Both in *Isthminia* and *Inia*, the posterior termination of the dentition and the anterior termination of the acoustic window occur in close proximity, whereas in *Pontoporia* these landmarks are separated by a large gap along the mandibular ramus. Lastly, for the scapula, *Isthminia* shares the most similarities with *Inia*, although the scapula is not known in the majority of fossil inioids, and it remains unpublished in the otherwise abundantly represented *Brachydelphis mazeasi* (e.g., MUSM 887). We note the presence of both a complete scapula and a humerus in the type specimen of *Incacetus broggii* Colbert, 1944 (AMNH 32656) from marine strata in the Ica Desert (likely the Pisco Formation, although it may derive from older strata) in

Peru. Both elements hint at inioid affinities for this taxon, from the Pisco Basin, which has previously been identified as a kentriodontid (*Muizon, 1988b*).

Taphonomy, body size, and ecomorphology

Isthminia was recovered from the type locality with the ventral surface of the skull exposed stratigraphic up, at the outcrop surface, directly overlying the mandibles, which were preserved slightly askew from the main axis of the skull, dorsal surface up (Fig. S1). Careful inspection of the surrounding quarry, prior to excavation, led to the recovery of 3 isolated teeth. The scapula was recovered within 1 m of the skull and jaws, mid-way through the excavation. Overall, the distribution of the skeletal elements at the type locality are similar to other fossil odontocetes in the same size, in similar depositional environments, and that have been recovered as associated skeletons (e.g., *Tanaka & Fordyce, 2015*). By comparison, there are generally far fewer postcranial elements preserved with the type specimen of *Isthminia* than might be expected, suggesting that most of the skeleton was likely eroded away from overlying rock.

The degree of disarticulation at the type locality corresponds to Articulation Stage 2 described by *Pyenson et al. (2014)* in their supplemental files, which matches the same articulation stage in *Boessenecker, Perry & Schmitt (2014)*. In terms of bone modification, there is no evidence of bite marks from marine macroscavengers, and we did not observe any of the phosphatization, fragmentation and polish described by *Boessenecker, Perry & Schmitt (2014)* for marine vertebrates from the Mio-Pliocene age Purisima Formation of California. In sum, these observations point to the type specimen of *Isthminia* representing a single individual skeleton showing little transport, slight disarticulation, and burial in a low energy depositional environment.

Using both the Platanistoidea and Delphinoidea body size equations from *Pyenson & Sponberg (2011)*, we calculated the total length of *Isthminia* between 284 and 287 cm, respectively, based on an estimate of the bizygomatic width of the skull by doubling the distance from the lateral surface of the zygomatic process to the midpoint of the mesethmoid. Assuming the type specimen represents a mature individual, this total length exceeds the largest values for *Inia* (LACM 19590 with TL = 221 cm) and *Pontoporia* (CAS 16529, with TL = 157 cm) from the adult specimens cited in *Pyenson & Sponberg (2011)*'s dataset, although we note that adult *Inia* and *Pontoporia* can attain lengths as large as 300 cm and 175 cm, respectively (*Nowak, 1999*). The reconstruction of *Isthminia*'s TL closely matches medium- to large-sized extant delphinoids, such as *Grampus griseus* (*Cuvier, 1812*), which has an average TL of 283 cm, based on 8 adult specimens in *Pyenson & Sponberg (2011)*'s dataset. Notably, *Isthminia* ranks among the largest of inioids, though it was slightly smaller than a similar estimate for *Ischyrorhynchus* (TL of 288–291 cm based on MACN 15135). *Saurocetes* spp., a *Pan-Inia* taxon, was likely much larger, but poorly known, based on incomplete material from the Ituzaingó Formation of Argentina for *Saurocetes gigas* (only known from a proximal fragment of a mandibular symphysis and isolated teeth), and mandibles and partial cranial specimens for *S. argentinus* from the late Miocene Ituzaingó,

Urumaco, and Solimões formations of Argentina, Venezuela, and Brazil, respectively (see *Gutstein, Cozzuol & Pyenson, 2014b*).

We also examined two relevant morphological ecomorphological indices: mandibular bluntness index (MBI) and proportional orbit size. First, we followed methods outlined by *Werth (2006)* and calculated a MBI value of 0.548 for *Isthminia*, which is greater than values for either *Inia* or *Pontoporia*. By comparison, the MBI value for *Isthminia* most closely resembles those for other delphinids reported by *Werth (2006)*. We also generated a simple metric to compare relative orbit size (ROS) among odontocetes, in an effort to better quantify the proportionally large orbits of *Isthminia*, especially with respect to *Inia* and *Pontoporia*. Using antorbital notch width to control for size (following *Pyenson & Sponberg, 2011*), we calculated a ROS value for *Isthminia* at 0.40 (Table 3). This value is larger than *Inia*, but smaller than *Meherrinia, Pontoporia*, and *Brachydelphis* spp. Comparisons among the dimensionless ROS indices do not immediately reveal any strong phylogenetic or ecologic structuring (Table 3), with *Isthminia* having a ROS in the same range as fossil and living marine odontocetes. It is entirely possible that ROS does not have the same importance in the sensory ecology of odontocetes as it does in other marine mammals that do not echolocate and therefore depend much more on visual prey detection (*Schusterman et al., 2000*; *Debey & Pyenson, 2013*).

The preponderance of occlusal wear facets on the apices of the lower and upper tooth crowns is not dissimilar from extant delphinioids, such as off-shore specimens of *Tursiops*, and fossil delphinidans such as *Lophocetus pappus*. Following *Loch & Simões-Lopes (2013)*, we scored 100% dental wear in the type and only specimen of *Isthminia*, with every tooth showing at least superficial apical tooth wear of the dental crown; only 2 out of 41 complete teeth in the dentition of the type specimen showed simultaneous wear in apical and lateral tooth facets. Although the percentage of simultaneous apical and lateral wear ranks comparatively low for *Loch & Simões-Lopes (2013)*'s dataset of delphinids from the coast of Brazil, the dominance of superficial dental crown corresponding to Index 1 is generally in line with similar modes from pelagic delphinids in their dataset. We note, however, that *Isthminia* has different overall tooth morphology and lower tooth counts as compared with stem and crown delphinoids, and fewer teeth than *Inia* and *Pontoporia*.

Overall, *Isthminia* shares some ecomorphological similarities with pelagic odontocetes, especially with delphinioids of comparable body sizes and MBI. In comparative studies of congeneric or closely related odontocetes with disparate habitat preferences (e.g., riverine or estuarine versus oceanic settings), *Monteiro-Filho, Monteiro & Reis (2002)* and *Galatius et al. (2011)* demonstrated associated morphological complexes with each habitat. Pelagic odontocetes, for example, tend to have rostra with less ventral inclination, possess facial regions that were dorsally and posteriorly expansive and more concave in lateral aspects. *Isthminia* is consistent with this pelagic characterization in having a rostral plane less ventrally inclined than either *Inia* or *Pontoporia*, and having a broad exposure of the maxillae posterior of the level of the external nares. Future work should quantify these features more broadly across fossil delphinidans in a way that can be comparable with *Galatius et al. (2011)*'s findings.

Environmental and ecological implications

Planktotrophy is the dominant feeding mode of both the benthonic and nektonic fossil invertebrate assemblages preserved in the Piña Facies (*Schwarzhans & Aguilera, 2013*; *O'Dea et al., 2007*) demonstrating high planktonic productivity. In contrast, modern Caribbean shelf shallow waters are dominated by low planktonic but high benthic productivity driven by autotrophic reef and seagrass growth (*O'Dea et al., 2007*). The shift from planktotrophic to autotrophic benthic communities took place across the Caribbean when the Isthmus of Panama formed ~3.5 Ma (*Jackson & O'Dea, 2013*). The presence of *Isthminia* and other predators including billfishes (*Fierstine, 1978*; J Velez-Juarbe, pers. comm., 2015), chondrichthyans (*Carrillo-Briceño et al., 2015*) and cetaceans such as kogiids (*Velez-Juarbe et al., 2015*), physeteroids (*Vigil & Laurito, 2014*), and delphinoids (J Velez-Juarbe, pers. comm., 2015), all with presumably high metabolic rates, corroborate further the presence of high planktonic productivity in the Piña Facies.

The source of high planktonic productivity is not yet resolved. Upwelled, nutrient-rich Pacific waters may have entered the Caribbean coast of Panama (*O'Dea et al., 2012*) through the remaining straits of the Central American Seaway (*Jackson & O'Dea, 2013*; *Coates & Stallard, 2013*; *Leigh, O'Dea & Vermeij, 2014*) in the late Miocene. High rates of cloning in cupuladriid bryozoans (*O'Dea & Jackson, 2009*), high variations in stable isotopes along skeletal profiles from gastropod shells (*Robbins et al., 2012*), and high variations in temperature-mediated zooid sizes (*O'Dea et al., 2007*) all suggest that strong seasonal upwelling was a dominate regime in this area. Alternatively, nutrients may have originated from more localized terrestrial runoff, as proposed for emergent platforms in present-day Colombia (*Montes et al., 2015*). However, reconciling the small watershed of the Isthmus of Panama with the geographic and stratigraphic extent of the Piña Facies (approximately 40–50 m thick) make it unlikely that high productivity levels observed throughout the facies could have been maintained solely from terrestrial input, even if higher rainfall and greater orogenic or volcanic activity in the late Miocene resulted in increased nutrient input from the proto-Isthmus. As such, it is unlikely that there were large rivers close to the area, further corroborating the hypothesis that *Isthminia* lived in a fully marine habitat.

The high abundance of benthic foraminifera assemblages with modern or ancient upper and middle bathyal depth ranges led *Collins et al. (1996)* to conclude that the Piña Facies of the Chagres Formation was deposited in deeper waters. *Collins et al. (1996)* suggested that the Piña Facies were preserved as the Central American Seaway deepened following the deposition of the underlying shallow-water Gatún Formation, and therefore represented the ephemeral formation of a fairly deep oceanic connection from the Pacific Ocean into the Caribbean Sea, prior to final closure of the Isthmus of Panama. This pattern of sediment deepening at the end of the Miocene, followed by shallowing and final closure of the Isthmus in the Late Pliocene, repeats itself across several basins along the Isthmus of Panama (*Coates et al., 2003*; *Coates et al., 2004*), pointing to pervasive regional eustatic sea level rise at the end of the Miocene (*Miller et al., 2005*) as a driver.

De Gracia et al. (2012) suggested that the extent of deepening at this time was extreme. They used the vast abundance of lanternfish (e.g., *Diaphus Eigenmann & Eigenmann, 1890*) recovered from the sediments (*Schwarzhans & Aguilera, 2013*) as evidence that the Piña Facies was deposited in up to 700 m of water depth (see File S2 for otolith abundance data from this unit, near the type locality). Although lanternfish do inhabit deeper waters during the day to avoid predation, they are well known to migrate into shallow waters at night to feed. Indeed, their otoliths are abundant in shallow water (<35 m) sediments in Bocas del Toro today. Thus, the presence of lanternfish, even in the great abundance observed in the Piña Facies is insufficient to assume deep-water deposition.

In a more recent study, *Hendy et al. (in press)* used molluscan, foraminferal, coral, and fish otolith assemblages, along with detailed sedimentological evidence, to conclude that the deepening event was considerably less pronounced. They suggested the deposition of the Piña Facies was around 125 m in depth, closely reflecting a previous estimate made by *Collins et al. (1999)* using corals and fish otoliths. Intense productivity or upwelling characteristic of the Piña Facies could have compressed thermoclines and compensation depths resulting in an apparent compression of the depth ranges of diagnostic taxa resulting in possibly anomalously deep estimates. The presence of a single specimen of *Isthminia* sheds little light on this palaeodepth discussion, except to note that modern day pelagic delphinoids concentrate around the neritic zone (*Benoit-Bird & Au, 2003*; *Gowans, Würsig & Karczmarski, 2007*; *Benoit-Bird & McManus, 2012*).

The evolutionary history of inioidea in the Americas

The fossil record of Inioidea reveals a far broader geographic distribution in the past than would be predicted from the extant ranges of *Inia* and *Pontoporia*. Fossil inioids outside of South America have predominantly been recovered from marine deposits representing nearshore depositional environments, although *Isthminia*'s recovery from rocks representing potentially a open ocean setting is consistent with ecomorphological traits that *Isthminia* shares with pelagic odontocetes alive today (Fig. 14). Although some freshwater *Pan-Inia* lineages from the late Miocene of Argentina may have been ∼4 m in total length, they are based on fragmentary remains (*Cozzuol, 2010*), and *Isthminia* is the largest marine inioid yet reported, in addition to being the only fossil inioid known from the Caribbean. Based on the available evidence, *Isthminia* occupied a high trophic level in a highly productive fully marine tropical Caribbean coastal ecosystem that predated the complete formation of the Panamanian Isthmus. Many of the bony fish species that are recorded in spectacular abundance from adjacent otolith assemblages in the Chagres Formation (File S2) may have formed a dominant portion of the prey resources for *Isthminia*, as they do for extant delphinids (see *Kelley & Motani, 2015*).

Hamilton et al. (2001) suggested that the marine ancestors of *Inia*, subsequent to their divergence from *Pontoporia*, invaded freshwater ecosystems of Amazonia during eustatic sea-level highs of the middle Miocene, and evolved freshwater habits prior to the subsequent drop in eustatic sea-level late in the Neogene. This proposed evolutionary scenario is entirely consistent with the late Miocene (Messinian) antiquity of *Isthminia*,

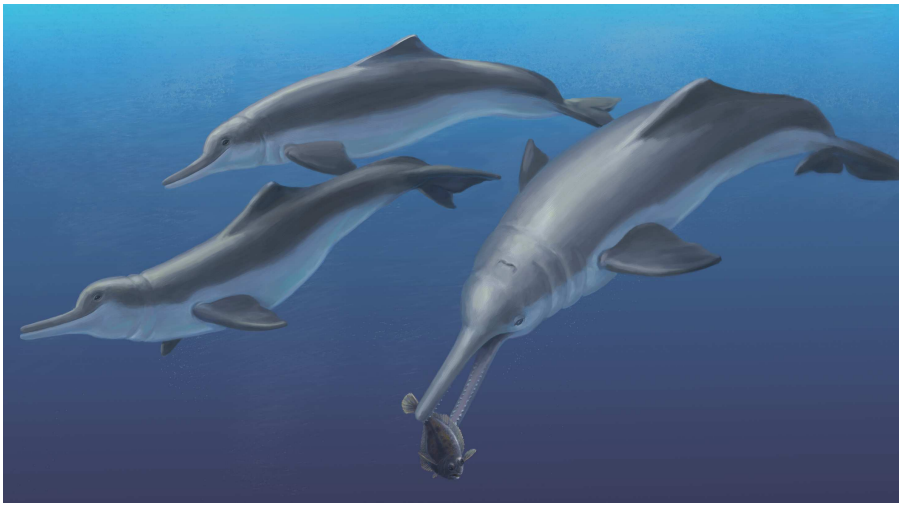

Figure 14 Reconstruction of *Isthminia*. Life reconstruction of *Isthminia panamensis*, feeding on a flatfish, which would have been abundant in the neritic zone of the late Miocene equatorial seas of Panama. Art by Julia Molnar.

which establishes a minimum boundary on its divergence with *Inia* (Fig. 15). Fossil remains attributable directly to *Inia* spp. have been reported from Pleistocene age freshwater deposits of the Rio Madeira Formation in Brazil (*Cozzuol, 2010*). An isolated *Pan-Inia* humerus from the late Miocene Ituzaingó Formation implies that this clade had already invaded turbid, obstructed shallow rivers and flooded forests typical of today's Amazonian freshwater ecosystems by this time, although this humerus may belong to extinct taxon more closely related to *Ischyrorhynchus* (*Gutstein et al., 2014a*).

The results of our phylogenetic analysis, however, cast some complexity on a simple scenario of marine-to-freshwater directionality given the phylogenetic placement of *Ischyrorhynchus*, from freshwater deposits of South America. Taken at face value, our analysis points to either two separate freshwater invasions in South America from marine ancestry at different times (one for *Ischyrorhynchus*, and another for *Inia*), or a single invasion with the origin at the unnamed clade of *Ischyrorhynchus* + *Isthminia* + *Inia*, with a marine re-invasion leading to *Isthminia* (Fig. 15). While the overwhelming marine ancestry for Inioidea is clear from the phylogenetic background of most odontocetes, there is no clear parsimonious argument for the directionality of marine-freshwater ecological transitions. *Geisler et al. (2011)* discussed such ecological complexity in considering *Hamilton et al. (2001)*'s scenario, pointing specifically to separate instances of overlapping geographic and ecological distributions between sympatric pairs of exclusively freshwater and estuarine to marine odontocete taxa: e.g., *Sotalia fluviatilis* (*Gervais, 1853*) with *Sotalia guianensis* (*Van Beneden, 1864*), both delphinids, in South America (*Cunha et al., 2005*; *Caballero et al., 2007*; *Gutstein, Cozzuol & Pyenson, 2014b*); and, prior to the former's extinction, *Lipotes vexillifer* and *Neophocaena phocoenoides* (*Cuvier, 1829*), a phocoenid, in China. These extant examples, along with the recent fossil discoveries of putatively marine odontocetes in freshwater depositional environments (*Bianucci et al.,*

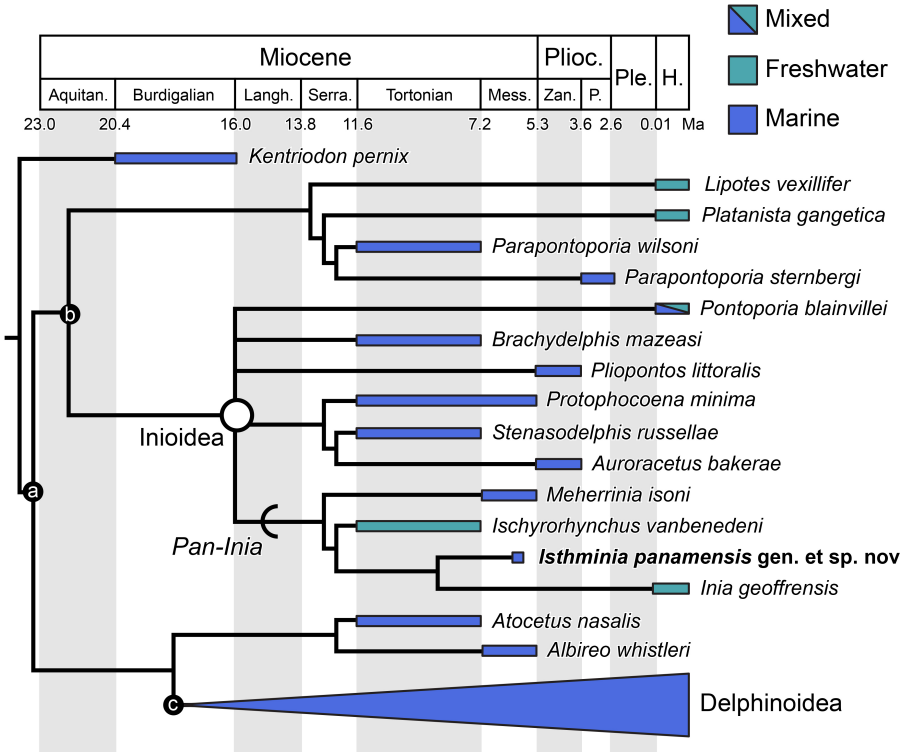

Figure 15 Stratigraphically calibrated phylogenetic tree of Inioidea. Time calibrated phylogenetic tree of select Delphinida, pruned from our consensus cladogram in Fig. 13, including *Isthminia*, with Delphinoidea collapsed. Stratigraphic range data derives from published accounts for each taxon, including global ranges. Geologic time scale based on *Cohen et al. (2013)*. Calibration for major nodes depths follow mean divergence date estimates by *McGowen, Spaulding & Gatesy* (*2009*: table 3) for the following clades: a, Delphinida (24.75 Ma); b, Inioidea + *Lipotes* (22.15 Ma); c, Delphinoidea (18.66 Ma); and Inioidea (in open white circle, 16.68 Ma). All minor node depths are graphical heuristics, and not intended to reflect actual divergence dates. Arc indicates stem-based clade, *Pan-Inia*. Ecological habitat preference is based on depositional environment or extant habitat. Abbreviations: Aquitan., Aquitanian; H., Holocene; Langh., Langhian; Mess., Messinian; P., Piacenzian; Ple., Pleistocene; Plioc., Pliocene; Serra., Serravallian; Zan., Zanclean.

2013; *Boessenecker & Poust, 2015*) suggest that freshwater invasions by marine odontocetes have happened frequently throughout the Neogene, in different continental margins, across major lineages, and, as our results suggest, perhaps within clades as well.

For South America, we conclude that marine odontocetes likely invaded freshwater ecosystems several times, with platanistids representing an initial invasion in the middle Miocene that ultimately disappeared, prior or subsequent to later a singular or repeated inioid invasions in the late Miocene. Future work, including new discoveries, will hopefully increase branch support for the phylogenetic arrangement of *Pan-Inia* (and basal inioids), and better refine this scenario for South American inioid evolution, and elsewhere. These evolutionary hypotheses may also be compared with diversification and selective extinction patterns for other vertebrate groups that invaded Amazonian freshwater ecosystems from marine ancestries (e.g., stingrays belonging to Potamotrygonidae *Garman, 1877*, see *Lovejoy, Bermingham & Martin, 1998*; croakers in the genus *Plagioscion Gill, 1861*,

see *Cooke, Chao & Beheregaray, 2012*), in conjunction with the timing of orogenetic events during the late Neogene (*Hoorn et al., 2010*). Lastly, comparative phylogenetic analyses of the physiology and functional morphology of odontocetes, and other possible marine tetrapod analogs that have overlapping ecological occupancy will also provide a better basis for evaluating adaptational hypotheses that explain their evolution (*Kelley & Pyenson, 2015*).

Anatomical Abbreviations

adif	anterior dorsal infraorbital foramen
alis	alisphenoid
ap	angular process of mandible
C	canine tooth
cp	coronoid process of mandible
cuneif	cuneiform
dsss	dorsal sagittal sinus sulcus
fplpts	fossa for the postorbital lobe of the pterygoid sinus
fr	frontal
gf	glenoid fossa of squamosal
I	incisor tooth or teeth
ju	jugal
la	lacrimal
Ma	mega-annum, period of 1 million years
max	maxilla
mc	maxillary crest
me	mesethmoid
mef	mental foramen or foramina
mf	mandibular foramen
ms	mandibular symphysis
na	nasal
nar	bony narial opening or naris
nuc	nuchal crest
pa	parietal
PC	postcanine tooth or teeth
pdif	posterior dorsal infraorbital foramen
pls	posterolateral sulcus of the premaxilla
pmax	premaxilla
pmaxf	premaxillary foramen
pms	posteromedial sulcus of the premaxilla
pmsf	premaxillary sac fossa
popf	postorbital process of the frontal
propf	preorbital process of the frontal
scap	scaphoid

socc	supraoccipital
sopf	supraorbital process of frontal
smf	suprameatal fossa
sq	squamosal
tc	temporal crest of the frontal
trap	trapezoid
uncif	unciform
vom	vomer
zpsq	zygomatic process of squamosal

Institutional Abbreviations

AMNH	Divisions of Paleontology and Vertebrate Zoology, American Museum of Natural History, New York, New York, USA.
CAS	Department of Ornithology and Mammalogy, California Academy of Sciences, San Francisco, California, USA.
CMM	Calvert Marine Museum, Solomons, Maryland, USA.
IRSNB	Institut royal des Sciences naturelles de Belgique, Brussels, Belgium.
LACM	Departments of Mammalogy and Vertebrate Paleontology, Natural History Museum of Los Angeles County, Los Angeles, California, USA.
MACN	Museo Argentino de Ciencias Naturales "Bernardino Rivadavia," Buenos Aires, Argentina.
MLP	Museo de La Plata, La Plata, Argentina.
MNHN	Muséum national d'Histoire naturelle, Paris, France.
MUSM	Museo de Historia Natural, Universidad Nacional Mayor San Marcos, Lima, Peru.
UCMP	University of California Museum of Paleontology, Berkeley, California, USA.
UF	Florida Museum of Natural History, Gainesville, Florida, USA.
USNM	Departments of Paleobiology and Vertebrate Zoology (Division of Mammals), National Museum of Natural History, Smithsonian Institution, Washington, D.C., USA.

ACKNOWLEDGEMENTS

Foremostly, we thank Felix Rodriguez, Owen McMillan and Eldredge Bermingham for their support. We would also like to thank Celideth DeLeon for her circumspect administrative help. We are grateful to the Government of Panama's Ministerio de Comercio e Industrias (MICI) and staff at STRI for assistance, including Santosh Jagadeeshan, Andrew Ugan and Carlos De Gracia, for logistical support with collecting and transporting the type specimen of *Isthminia*, which was collected and exported with permits from the MICI. We thank Steven Jabo and Peter Kroehler (USNM) for technical assistance with preparation of the type specimen. We also thank Tomas Hrbek, an anonymous reviewer, and Academic Editor Mark Young for helpful comments on the manuscript. For insightful

discussions and access to unpublished data, we thank Stephen J. Godfrey, Olivier Lambert, Mizuki Murakami, R. Ewan Fordyce, James G. Mead, Charles W. Potter, David J. Bohaska, and Alexander J. Werth. We also thank James F. Parham for suggestions and comments on many drafts of the manuscript. We also thank David J. Bohaska, Charles W. Potter, John J. Ososky, and James G. Mead (all USNM), John R. Nance and Stephen J. Godfrey (CMM), Rodolfo S. Gismondi (MUSM), Christine Argot, Guillaume Billet, and Christian de Muizon (all MNHN), Patricia A. Holroyd (UCMP), Marcelo Ruguero (MLP), Alejandro Kramarz (MACN), and John Flynn, Ruth O'Leary, Nancy B. Simmons, and Neil Duncan (all AMNH), and staff at the Instituto de Desenvolvimento Sustentável Mamirauá in Tefé, Brazil, who all provided access to collections under their care. We are grateful for the support of NMNH Imaging, including the late Donald Hurlbert, James Di Loreto, Brittany Hance, and Kristen N. Quarles, for photography of the type specimen of *Isthminia*. We thank Tatjana Dzambazova (Autodesk), Antonije Velevski and Ralph Wiedemeier for website assistance with the 3D model of *Isthminia*, Ping Fu (3D Systems) and Günter Waibel, Adam Metallo, Vincent Rossi, and Jon Blundell of the Smithsonian's Digitization Program Office for their support with 3D digitization. We are grateful to Esteban Pacheco for printing and donating a 3D model of *Isthminia*. We also thank Tina Tennessen for her timely editorial skills, and the input of Lauren O'Regan and Loretta Cooper (all at USNM). Orangel Aguilera kindly gave permission to use his fish otolith data from the Chagres Formation. Marcelo Viana and Orangel Aguilera kindly allowed us to use fish images in preliminary drafts of *Isthminia*'s reconstruction. We are indebted to the generosity and expertise of Laurel Collins, for help with the stratigraphy and age of the Chagres Formation, and we thank Austin Hendy for the base map in Fig. 2. Lastly, we thank Julia Molnar for her creative and careful execution on the life reconstructions of *Isthminia*.

ADDITIONAL INFORMATION AND DECLARATIONS

Funding

The research of NDP was funded by the Smithsonian Institution, its Remington Kellogg Fund, and with support from the Basis Foundation. This project was also partially funded by an NSF EAR Postdoctoral Fellowship (1249920) to JVJ and NSF PIRE (0966884). Funding from CONICYT, Becas Chile, Departamento de Postgrado y Postítulo of the Vicerrectoría de Asuntos Académicos of Universidad de Chile supported CSG. This research was also supported financially by the National System of Investigators (SNI) of the National Secretariat for Science, Technology and Innovation of Panama (SENACYT) and a NSF Collaborative Research award (1325379) to AO. The funders had no role in study design, data collection and analysis, decision to publish, or preparation of the manuscript.

Grant Disclosures

The following grant information was disclosed by the authors:
Smithsonian Institution.
NSF EAR Postdoctoral Fellowship: 1249920.
NSF PIRE: 0966884.

CONICYT.
National System of Investigators (SNI).
NSF Collaborative Research award: 1325379.

Competing Interests

Nicholas D. Pyenson is an Academic Editor for PeerJ. Jorge Velez-Juarbe is an employee of Natural History Museum of Los Angeles County and Nicholas D. Pyenson and Holly Little are employees of National Museum of Natural History, Smithsonian Institution. Aaron O'Dea is an employee of Smithsonian Tropical Research Institute.

Author Contributions

- Nicholas D. Pyenson, Jorge Vélez-Juarbe, Carolina S. Gutstein and Aaron O'Dea conceived and designed the experiments, performed the experiments, analyzed the data, contributed reagents/materials/analysis tools, wrote the paper, prepared figures and/or tables, reviewed drafts of the paper.
- Holly Little performed the experiments, analyzed the data, wrote the paper, prepared figures and/or tables, reviewed drafts of the paper.
- Dioselina Vigil conceived and designed the experiments, performed the experiments, reviewed drafts of the paper.

Field Study Permissions

The following information was supplied relating to field study approvals (i.e., approving body and any reference numbers):

Fossil material was collected and exported under the Government of the Republic of Panama's Ministerio de Comercio e Industrias (MICI number DNRM-MC-074-11).

Data Availability

The following information was supplied regarding the deposition of related data:

Full resolution 3D models and original CT data are available online at Smithsonian X 3D (http://3d.si.edu) and archived, along with supplemental data, in Zenodo (https://zenodo.org/record/27214) at the following DOI: 10.5281/zenodo.27214.

New Species Registration

The following information was supplied regarding the registration of a newly described species:

Isthminia
urn:lsid:zoobank.org:act:83F6A9B4-289D-45DE-A3D1- C361DAAAF973
Isthminia panamensis
urn:lsid:zoobank.org:act:A5C706B6-E0B6-43E5-A65C-E6FE0B2BDF1A.

Supplemental Information

Supplemental information for this article can be found online at http://dx.doi.org/10.7717/peerj.1227#supplemental-information.

REFERENCES

Abel O. 1905. Les Odontocètes du Boldérien (Miocène supérieur) des environs d'Anvers. *Mémoires du Musée royal d'Histoire naturelle de Belgique* **3**:1–155.

Aguirre-Fernández G, Fordyce RE. 2014. *Papahu taitapu*, gen. et sp. nov., an early Miocene stem odontocete (Cetacea) from New Zealand. *Journal of Vertebrate Paleontology* **34**:195–210 DOI 10.1080/02724634.2013.799069.

Allen GM. 1921. A new fossil cetacean. *Bulletin of the Museum of Comparative Zoology* **65**:1–14.

Allen GM. 1941. A fossil river dolphin from Florida. *Bulletin of the Museum of Comparative Zoology* **89**:1–24.

Ameghino F. 1891. Caracteres diagnosticos de cincuenta especies nuevas de mamiferos fosiles argentinos. *Revista Argentina de Historia Natural* **1**:129–167.

Arnason U, Gullberg A, Janke A. 2004. Mitogenomic analyses provide new insights into cetacean origin and evolution. *Gene* **333**:27–34 DOI 10.1016/j.gene.2004.02.010.

Barnes LG. 1984. Fossil odontocetes (Mammalia: Cetacea) from the Almejas Formation, Isla Cedros, Mexico. *PaleoBios* **42**:1–46.

Barnes LG. 1985a. Fossil pontoporiid dolphins (Mammalia: Cetacea) from the Pacific coast of North America. *Contributions in Science* **363**:1–34.

Barnes LG. 1985b. The late Miocene dolphin *Pithanodelphis* Abel, 1905 (Cetacea: Kentriodontidae) from California. *Contributions in Science* **367**:1–27.

Benoit-Bird KJ, Au WW. 2003. Prey dynamics affect foraging by a pelagic predator (*Stenella longirostris*) over a range of spatial and temporal scales. *Behavioral Ecology and Sociobiology* **53**:364–373 DOI 10.1007/s00265-003-0585-4.

Benoit-Bird KJ, McManus MA. 2012. Bottom-up regulation of a pelagic community through spatial aggregations. *Biology Letters* **8**:813–816 DOI 10.1098/rsbl.2012.0232.

Bianucci G, Lambert O, Salas-Gismondi R, Tejada J, Pujos F, Urbina M, Antoine PO. 2013. A Miocene relative of the Ganges River dolphin (Odontoceti, Platanistidae) from the Amazonian Basin. *Journal of Vertebrate Paleontology* **33**:741–745 DOI 10.1080/02724634.2013.734888.

Blainville HMD de. 1817. Les quadrupèdes, les cétacés et les animaux fossiles. In: Desmarest AG, ed. *Nouveau dictionnaire d'histoire naturelle, appliquée aux arts, à l'agriculture, à l'économie rurale et domestique, à la médecine, etc. par une societé de naturalistes et d'agriculteurs*, vol. 9. Paris, France: Déterville, 1–624.

Boessenecker RW, Perry FA, Schmitt JG. 2014. Comparative taphonomy, taphofacies, and bonebeds of the Mio-Pliocene Purisima Formation, central California: strong physical control on marine vertebrate preservation in shallow marine settings. *PLoS ONE* **9**:e91419 DOI 10.1371/journal.pone.0091419.

Boessenecker RW, Poust AW. 2015. Freshwater occurrence of the extinct dolphin *Parapontoporia* (Cetacea: Lipotidae) from the upper Pliocene nonmarine Tulare Formation of California. *Palaeontology* **58**:489–496 DOI 10.1111/pala.12153.

Bolli HM. 1957. Planktonic foraminifera from the Oligocene-Miocene Cipero and Lengua formations of Trinidad, B.W.I. *Bulletin of the United States National Museum* **215**:97–123.

Bolli HM, Bermúdez PJ. 1965. Zonation based on planktonic foraminifera of middle Miocene to Pliocene warm-water sediments. *Boletín Informative Asociación Venezolana de Geología Mineraría y Petróleo* **8**:119–149.

Brisson MJ. 1762. *Regnum animale in Classes IX distributum, sive synopsis methodica sistens generalem animalium distributionem in Classes IX, et duarum primarum Classium,*

Quadrupedum scilicet & Cetaceorum, particulare divisionem in Ordines, Sectiones, Genera, et Species. Paris: T. Haak, 296 pp.

Burmeister G. 1871. On *Saurocetes argentinus* a new type of Zeuglodontidae. *Annals and Magazine of Natural History* **6**:51–55 DOI 10.1080/00222937108696312.

Burmeister G. 1885. Examen critico de los mamiferos y reptiles fosiles denominados por D. Augusto Bravard y mencionados en su obra precedente. *Annales del Museo Nacional de Buenos Aires* **3**:93–174.

Caballero S, Trujillo F, Vianna JA, Barrios-Garrido H, Montiel MG, Beltrán-Pedreros S, Marmontel M, Santos MC, Rossi-Santos M, Santos FR, Baker CS. 2007. Taxonomic status of the genus *Sotalia*: species level ranking for "tucuxi" (*Sotalia fluviatilis*) and "costero" (*Sotalia guianensis*) dolphins. *Marine Mammal Science* **23**:358–386 DOI 10.1111/j.1748-7692.2007.00110.x.

Cantino PD, De Queiroz K. 2014. *PhyloCode: a phylogenetic code of biological nomenclature*. Version 4c. Ohio University. *Available at http://www.ohiou.edu/phylocode*.

Carrillo-Briceño JD, De Gracia C, Pimiento C, Aguilera OA, Kindlimann R, Santamarina P, Jaramillo C. 2015. A new late Miocene chondrichthyan assemblage from the Chagres Formation, Panama. *Journal of South American Earth Sciences* **60**:56–70 DOI 10.1016/j.jsames.2015.02.001.

Cassens I, Vicario S, Waddell VG, Balchowsky H, Van Belle D, Ding W, Fan C, Lal Mohan RS, Simões-Lopes PC, Bastida R, Meyer A, Stanhope MJ, Milinkovitch MC. 2000. Independent adaptation to riverine habitats allowed survival of ancient cetacean lineages. *Proceedings of the National Academy of Sciences of the United States of America* **97**:11343–11347 DOI 10.1073/pnas.97.21.11343.

Chapman F, Parr WJ, Collins AC. 1934. Tertiary foraminifers of Victoria, Australia: the Balcombian deposits of Port Philip (Pt. III). *Journal of the Linnean Society of London* **38**:553–577 DOI 10.1111/j.1096-3642.1934.tb00996.x.

Coates AG, Aubry MP, Berggren WA, Collins LS, Kunk M. 2003. Early Neogene history of the Central American arc from Bocas del Toro, western Panama. *Geological Society of America Bulletin* **115**:271–287 DOI 10.1130/0016-7606(2003)115<0271:ENHOTC>2.0.CO;2.

Coates AG, Collins LS, Aubry MP, Berggren WA. 2004. The geology of the Darien, Panama, and the late Miocene-Pliocene collision of the Panama arc with northwestern South America. *Geological Society of America Bulletin* **116**:1327–1344 DOI 10.1130/B25275.1.

Coates AG, Stallard RF. 2013. How old is the Isthmus of Panama? *Bulletin of Marine Science* **89**:801–813 DOI 10.5343/bms.2012.1076.

Cohen KM, Finney SC, Gibbard PL, Fan JX. 2013. The ICS international chronostratigraphic chart. *Episodes* **36**:199–204.

Colbert EH. 1944. A new fossil whale from the Miocene of Peru. *Bulletin of the American Museum of Natural History* **83**:199–216.

Collins LS, Aguilera O, Borne PF, Cairns SD. 1999. A paleoenvironmental analysis of the Neogene of Caribbean Panama and Costa Rica using several Phyla. Un análisis paleoambiental del Neogeno del Caribe de Panamá y Costa Rica utilizando varios Phyla. *Bulletins of American Paleontology* **357**:81–87.

Collins LS, Coates AG, Berggren WA, Aubry MP, Zhang J. 1996. The late Miocene Panama isthmian strait. *Geology* **24**:687–690 DOI 10.1130/0091-7613(1996)024<0687:TLMPIS>2.3.CO;2.

Committee on Taxonomy. 2014. List of marine mammal species and subspecies. Society for Marine Mammalogy. *Available at www.marinemammalscience.org* (accessed 10 July 2015).

Cooke GM, Chao NL, Beheregaray LB. 2012. Marine incursions, cryptic species and ecological diversification in Amazonia: the biogeographic history of the croaker genus *Plagioscion* (Sciaenidae). *Journal of Biogeography* **39**:724–738 DOI 10.1111/j.1365-2699.2011.02635.x.

Cooper LN, Berta A, Dawson SD, Reidenberg JS. 2007. Evolution of hyperphalangy and digit reduction in the cetacean manus. *The Anatomical Record* **290**:654–672 DOI 10.1002/ar.20532.

Cozzuol MA. 1989. Una nueva especie de *Saurodelphis* Burmeiter, 1891 (Cetácea: Iniidae) del "Mesopotamiense" (Mioceno Tardio-Plioceno Temprano) de la provincia de Entre Rios, Argentina. *Ameghiniana* **25**:39–45.

Cozzuol MA. 1996. The records of the aquatic mammals in Southern South America. *Munchner Geowissenschaftliche Abhandlungen* **30**:321–342.

Cozzuol MA. 2010. Fossil record and the evolutionary history of Inioidea. In: Ruiz-Garcia M, Shostell JM, eds. *Biology, evolution and conservation of river dolphins within South America and Asia*. Hauppage: Nova Science Publishers, 193–221.

Cunha HA, Da Silva VMF, Lailson-Brito J, Santos MC de O, Flores PAC, Martin AR, Azevedo AF, Fragoso ABL, Zanelatto RC, Sole-Cava AM. 2005. Riverine and marine ecotypes of *Sotalia* dolphins are different species. *Marine Biology* **148**:449–457 DOI 10.1007/s00227-005-0078-2.

Cuvier G. 1812. Rapport fait à la classe des Sciences mathématiques et physiques, sur divers Cétacés pris sur les côtes de France, pricipalement sur ceux qui sont échoués près de Paimpol, le 7 janvier 1812. *Annales du Muséum d'Histoire Naturelle* **19**:13–14.

Cuvier G. 1829. *Le règne animal distribué d'après son organisation, pour servir de base à l'histoire naturelle des animaux et d'introduction à l'anatomie comparée*. Vol. 1. Paris: Chez Déterville Tom, 291.

Debey LB, Pyenson ND. 2013. Osteological correlates and phylogenetic analysis of deep diving in living and extinct pinnipeds: what good are big eyes? *Marine Mammal Science* **29**:48–83 DOI 10.1111/j.1748-7692.2011.00545.x.

De Gracia C, Carrillo-Briceño J, Schwarzhans W, Jaramillo C. 2012. An exceptional marine fossil fish assemblage reveals a highly productive deep-water environment in the Central American Seaway during the late Miocene [Abstract 164]. *Geological Society of America Abstracts with Programs* **44**.

d'Orbigny A. 1834. Notice sur un nouveau genre de cétacé des rivières du centre de l'Amérique méridionale. *Nouveau Annales du Musée d'Histoire Naturel de Paris* **3**:28–36.

Eigenmann CH, Eigenmann RS. 1890. Additions to the fauna of San Diego. *Proceedings of the California Academy of Sciences of the United States of America* **3(Series 2)**:1–24.

Fierstine HL. 1978. A new marlin, *Makaira panamensis* from the Late Miocene of Panama. *Copeia* **1978**:1–11 DOI 10.2307/1443812.

Flower WH. 1867. Description of the skeleton of *Inia geoffrensis* and of the skull of *Pontoporia blainvillii*, with remarks on the systematic position on these animals in the order Cetacea. *Transactions of the Zoological Society of London* **6**:87–116 DOI 10.1111/j.1096-3642.1867.tb00572.x.

Fordyce RE. 2002. *Simocetus rayi* (Odontoceti: Simocetidae, New Family): a bizarre new archaic Oligocene dolphin from the eastern North Pacific. *Smithsonian Contributions to Paleobiology* **93**:185–222.

Fordyce RE. 2009. Cetacean fossil record. In: Perrin WF, Würsig B, Thewissen JGM, eds. *Encyclopedia of marine mammals*. Second edition. Amsterdam: Elsevier, 207–215.

Fraser FC, Purves PE. 1960. Hearing in cetaceans. Evolution of the accessory air sacs and the structure and function of the outer and middle ear in recent cetaceans. *Bulletin of the British Museum of Natural History, Zoology* **7**:1–140.

Galatius A, Berta A, Frandsen MS, Goodal RNP. 2011. Interspecific variation of ontogeny and skull shape among porpoises (Phocoenidae). *Journal of Morphology* **272**:136–148 DOI 10.1002/jmor.10900.

Garman SW. 1877. On the pelvis and external sexual organs of Selachians, with especial reference to the new genera *Potamotrygon* and *Disceus*. *Proceedings of the Boston Society of Natural History* **19**:197–215.

Gatesy J, Geisler JH, Chang J, Buell C, Berta A, Meredith RW, Springer MS, McGowen MR. 2013. A phylogenetic blueprint for a modern whale. *Molecular Phylogenetics and Evolution* **66**:479–506 DOI 10.1016/j.ympev.2012.10.012.

Geisler JH, Godfrey SJ, Lambert O. 2012. A new genus and species of late Miocene inioid (Cetacea, Odontoceti) from the Meherrin River, North Carolina, USA. *Journal of Vertebrate Paleontology* **32**:198–211 DOI 10.1080/02724634.2012.629016.

Geisler JH, McGowen MR, Yang G, Gatesy J. 2011. A supermatrix analysis of genomic, morphological, and paleontological data from crown Cetacea. *BMC Evolutionary Biology* **11**:112 DOI 10.1186/1471-2148-11-112.

Geisler JH, Sanders AE. 2003. Morphological evidence for the phylogeny of Cetacea. *Journal of Mammalian Evolution* **10**:23–129 DOI 10.1023/A:1025552007291.

Gervais P. 1853. Remarques sur les mammifères marins qui fréquentent les côtes de la France et plus particulièrement sur une novelle espèce de dauphins propre á la Méditerranée. *Bulletin Société Centrale d'Agriculture et des Comices Agricoles du Département de l'Hérault, Montpelier* **40**:140–155.

Gervais P. 1855. *Histoire Naturelle des Mammifères avec l'indication de leurs moeurs et de leurs rapports avec les arts le commerce et l'agriculture*. Paris: L. Curmer, 1–344.

Gervais P, d'Orbigny A. 1844. Mammalogie. *Extraits des procès-verbaux des séances (Société philomathique de Paris). Séance de 27 avril* **1844**:38–40.

Gibson ML, Geisler JH. 2009. A new Pliocene dolphin (Cetacea: Pontoporiidae), from the Lee Creek Mine, North Carolina. *Journal of Vertebrate Paleontology* **29**:966–971 DOI 10.1671/039.029.0307.

Gill T. 1861. Synopsis of the subfamily of Percinae. *Proceedings of the Academy of Natural Sciences Philadelphia* **1861**:44–52.

Gingerich PD. 2005. Cetacea. In: Rose KD, Archibald JD, eds. *Placental mammals: origin, timing, and relationships of the major extant clades*. Baltimore: Johns Hopkins University Press, 234–252.

Godfrey SJ, Barnes LG. 2008. A new genus and species of late Miocene pontoporiid dolphin (Cetacea: Odontoceti) from the St. Marys Formation in Maryland. *Journal of Vertebrate Paleontology* **28**:520–528 DOI 10.1671/0272-4634(2008)28[520:ANGASO]2.0.CO;2.

Gowans S, Würsig B, Karczmarski L. 2007. The social structure and strategies of delphinids: predictions based on an ecological framework. *Advances in Marine Biology* **53**:195–294.

Gray JE. 1846. On the cetaceous animals. In: Richardson J, Gray JE, eds. *The zoology of the voyage of H. M. S. Erebus and Terror, under the command of Capt. Sir J. C. Ross, R. N., F. R. S., During the Years 1839 to 1843*. London: E. W. Janson, 13–53.

Gutstein CS, Cozzuol MA, Pyenson ND. 2014b. The antiquity of riverine adaptations in Iniidae (Cetacea, Odontoceti) documented by a humerus from the late Miocene of the Ituzaingó Formation, Argentina. *The Anatomical Record* **297**:1096–1102 DOI 10.1002/ar.22901.

Gutstein C, Cozzuol M, Vargas AO, Suárez M, Schultz C. 2009. Patterns of skull variation of *Brachydelphis* (Cetacea, Odontoceti, Pontoporiidae) from South-Easthern Pacific Neogene. *Journal of Mammalogy* **90**:504–519 DOI 10.1644/07-MAMM-A-081.1.

Gutstein CS, Figueroa-Bravo CP, Pyenson ND, Yury-Yañez RE, Cozzuol MA, Canals M. 2014a. High frequency echolocation, ear morphology, and the marine–freshwater transition: a comparative study of extant and extinct toothed whales. *Palaeogeography, Palaeoclimatology, Palaeoecology* **400**:62–74 DOI 10.1016/j.palaeo.2014.01.026.

Gutstein CS, Horwitz FE, Valenzuela-Toro AM, Figueroa-Bravo CP. 2015. Cetáceos fósiles de Chile: context evolutivo y paleobiogeográfico. *Publicación Ocasional del Museo Nacional de Historia Natural, Chile* **63**:339–387.

Hamilton H, Caballero S, Collins AG, Brownell RL. 2001. Evolution of river dolphins. *Proceedings of the Royal Society of London B: Biological Sciences* **268**:549–556 DOI 10.1098/rspb.2000.1385.

Hendy AJW, Jones D, De Gracia D, Velez-Juarbe J. Paleoecology of the Chagres Formation (latest Miocene) of Panama: reinterpreting the paleoenvironment of a vertebrate-rich marine fauna. *Journal of Geology* In Press.

Hoorn C, Wesselingh FP, Steege H, Bermudez MA, Mora A, Sevink J, Sanmartín I, Sanchez-Meseguer A, Anderson CL, Figueiredo JP, Jaramillo J, Riff D, Negri FR, Hooghiemstra H, Lundberg J, Stadler T, Särkinen T, Antonelli A. 2010. Amazonia through time: Andean uplift, climate change, landscape evolution, and biodiversity. *Science* **330**:927–931 DOI 10.1126/science.1194585.

Hrbek T, Da Silva VMF, Dutra N, Gravena W, Martin AR, Farias IP. 2014. A new species of river dolphin from Brazil or: how little do we know our biodiversity. *PLoS ONE* **9**:e83623 DOI 10.1371/journal.pone.0083623.

IUCN (International Union for Conservation of Nature). 2013. *Inia geoffrensis. The IUCN Red List of threatened species*. Version 2014.

Jackson JBC, O'Dea A. 2013. Timing of the oceanographic and biological isolation of the Caribbean sea from the tropical eastern Pacific Ocean. *Bulletin of Marine Science* **89**:779–800.

Joyce WG, Parham JF, Gauthier J. 2004. Developing a protocol for the conversion of rank-based taxon names to phylogenetically defined clade names, as exemplified by turtles. *Journal of Paleontology* **78**:989–1013 DOI 10.1666/0022-3360(2004)078<0989:DAPFTC>2.0.CO;2.

Kelley NP, Motani R. 2015. Trophic convergence drives morphological convergence in marine tetrapods. *Biology Letters* **11(1)**:20140709 DOI 10.1098/rsbl.2014.0709.

Kelley NP, Pyenson ND. 2015. Evolutionary innovation and ecology in marine tetrapods from the Triassic to the Anthropocene. *Science* **348**:aaa3716 DOI 10.1126/science.aaa3716.

Kellogg R. 1927. *Kentriodon pernix*, a Miocene porpoise from Maryland. *Proceedings of the United States National Museum* **69**:1–14 DOI 10.5479/si.00963801.69-2645.1.

Kellogg R. 1955. Three Miocene porpoises from the Calvert Cliffs, Maryland. *Proceedings of the United States National Museum* **105**:101–154 DOI 10.5479/si.00963801.105-3354.101.

Kellogg R. 1966. A new odontocete from the Calvert Miocene of Maryland. *Proceedings of the United States National Museum* **247**:99–101.

Lambert O, De Muizon C. 2013. A new long-snouted species of the Miocene pontoporiid dolphin *Brachydelphis* and a review of the Mio-Pliocene marine mammal levels in the Sacaco Basin, Peru. *Journal of Vertebrate Paleontology* **33**:709–721 DOI 10.1080/02724634.2013.743405.

Lambert O, Post K. 2005. First European pontoporiid dolphins (Mammalia: Cetacea, Odontoceti) from the Miocene of Belgium and The Netherlands. *Deinsea* **11**:7–20.

Lebeck HJ. 1801. *Delphinus gangeticus* beschrieben von Heinrich Julius Lebeck zu Trankenbar. In: *Der Gesellschaft naturforschender Freunde zu Berlin Neue Schriften*. vol. 3. 280–282 Tab. II.

Leigh EG, O'Dea A, Vermeij GJ. 2014. Historical biogeography of the Isthmus of Panama. *Biological Reviews* **89**:148–172 DOI 10.1111/brv.12048.

Lilljeborg W. 1861. Supplément au mémoire sur les genres *Liriope* et *Peltogaster*, H. Rathke. *Nova Acta Regiae Societatis Scientiarum Upsaliensis, Seriei Tertiae* **3**:74–102.

Linnaeus C. 1758. *Systema naturae per regna tria naturae, secundum classes, ordines, genera, species, cum characteribus, differentiis, synonymis, locis. Tomus 1, Editio decima, reformata*. Stockholm: Laurentii Salvii, 1–824.

Loch C, Simões-Lopes PC. 2013. Dental wear in dolphins (Cetacea: Delphinidae) from southern Brazil. *Archives of Oral Biology* **58**:134–141 DOI 10.1016/j.archoralbio.2012.08.002.

Lovejoy NR, Bermingham E, Martin AP. 1998. Marine incursion into South America. *Nature* **396**:421–422 DOI 10.1038/24757.

May-Collado LJ, Agnarsson I. 2006. Cytochrome b and Bayesian inference of whale phylogeny. *Molecular Phylogenetics and Evolution* **38**:344–354 DOI 10.1016/j.ympev.2005.09.019.

McGowen MR, Spaulding M, Gatesy J. 2009. Divergence date estimation and a comprehensive molecular tree of extant cetaceans. *Molecular Phylogenetics and Evolution* **53**:891–906 DOI 10.1016/j.ympev.2009.08.018.

Mead JG, Fordyce RE. 2009. The therian skull: a lexicon with emphasis on the odontocetes. *Smithsonian Contributions to Zoology* **627**:1–248 DOI 10.5479/si.00810282.627.

Messenger SL, McGuire JA. 1998. Morphology, molecules, and the phylogenetics of cetaceans. *Systematic Biology* **47**:90–124 DOI 10.1080/106351598261058.

Miller Jr GS. 1918. A new river dolphin from China. *Smithsonian Miscellaneous Collections* **68**:1–12.

Miller KG, Kominz MA, Browning JV, Wright JD, Mountain GS, Katz ME, Sugarman PJ, Cramer BS, Christie-Blick N, Pekar SF. 2005. The Phanerozoic record of global sea-level change. *Science* **310**:1293–1298 DOI 10.1126/science.1116412.

Monteiro-Filho EL, Monteiro LR, Reis SF. 2002. Skull shape and size divergence in dolphins of the genus *Sotalia*: a tridimensional morphometric analysis. *Journal of Mammalogy* **83**:125–134 DOI 10.1644/1545-1542(2002)083<0125:SSASDI>2.0.CO;2.

Montes C, Cardona A, Jaramillo C, Pardo A, Silva JC, Valencia V, Ayala C, Pérez-Angel LC, Rodriguez-Parra LA, Ramirez V, Niño H. 2015. Middle Miocene closure of the Central American Seaway. *Science* **348**:226–229 DOI 10.1126/science.aaa2815.

Morgan GS. 1994. Miocene and Pliocene marine mammal faunas from the Bone Valley Formation of Central Florida. In: Berta A, Deméré TA, eds. *Contributions in marine mammal paleontology Honoring Frank C. Whitmore, Jr*, *Proceedings of the San Diego society of natural history,* vol. 29. 239–268.

Muizon C de. 1983. *Pliopontos littoralis* un nouveau Platanistidae Cetacea du Pliocène de la côte péruvienne. *Comptes Rendus de l'Academie des Sciences Paris Série II* **296**:1101–1104.

Muizon C de. 1984. Les vertébrés fossiles de la Formation Pisco (Pérou) Deuxième partie: les Odontocètes (Cetacea, Mammalia) du Pliocéne inférieur de Sud Sacaco. *Travaux de l'Institut français d' Études andines* **27**:1–188.

Muizon C de. 1988a. Les relations phylogénétiques des Delphinida (Cetacea, Mammalia). *Annales de Paleontologie* **74**:159–227.

Muizon C de. 1988b. Les vertébrés fossiles de la Formation Pisco (Pérou) Troisième partie: Les Odontocètes (Cetacea: Mammalia) du Miocène. *Travaux de l'Institut français d'Études andines* **42**:1–244.

Murakami M, Shimada C, Hikida Y, Soeda Y, Hirano H. 2014. *Eodelphis kabatensis*, a new name for the oldest true dolphin *Stenella kabatensis* Horikawa, 1977 (Cetacea, Odontoceti, Delphinidae), from the upper Miocene of Japan, and the phylogeny and paleobiogeography of Delphinoidea. *Journal of Vertebrate Paleontology* **34**:491–511 DOI 10.1080/02724634.2013.816720.

Nikaido M, Matsuno F, Hamilton H, Brownell Jr RL, Cao Y, Ding W, Zuoyan Z, Shedlock AM, Fordyce RE, Hasegawa M, Okada N. 2001. Retroposon analysis of major cetacean lineages: the monophyly of toothed whales and the paraphyly of river dolphins. *Proceedings of the National Academy of Sciences of the United States of America* **1998**:7384–7389 DOI 10.1073/pnas.121139198.

Nowak RM. 1999. *Walker's mammals of the World*. Baltimore: Johns Hopkins University Press.

O'Dea A, Hoyos N, Rodríguez F, Degracia B, De Gracia C. 2012. History of upwelling in the Tropical Eastern Pacific and the paleogeography of the Isthmus of Panama. *Palaeogeography, Palaeoclimatology, Palaeoecology* **348**:59–66 DOI 10.1016/j.palaeo.2012.06.007.

O'Dea A, Jackson J. 2009. Environmental change drove macroevolution in cupuladriid bryozoans. *Proceedings of the Royal Society B: Biological Sciences* **276**:3629–3634 DOI 10.1098/rspb.2009.0844.

O'Dea A, Jackson JB, Fortunato H, Smith JT, D'Croz L, Johnson KG, Todd JA. 2007. Environmental change preceded Caribbean extinction by 2 million years. *Proceedings of the National Academy of Sciences of the United States of America* **104**:5501–5506 DOI 10.1073/pnas.0610947104.

Perrin WF. 1975. Variation of spotted and spinner porpoise (genus *Stenella*) in the eastern Pacific and Hawaii. *Bulletin of the Scripps Institution of Oceanography of the University of California* **21**:1–206.

Pilleri G, Gihr M. 1977. Observations on the Bolivian (*Inia boliviensis* d'Orbigny, 1834) and the Amazon bufeo (*Inia geoffrensis* de Blainville, 1817) with description of a new subspecies (*Inia geoffrensis humboldtiana*). *Investigations on Cetacea* **8**:11–76.

Pyenson ND. 2009. Requiem for *Lipotes*: an evolutionary perspective on marine mammal extinction. *Marine Mammal Science* **25**:714–724 DOI 10.1111/j.1748-7692.2008.00266.x.

Pyenson ND, Gutstein CS, Parham JF, Le Roux JP, Chavarría CC, Little H, Metallo A, Rossi V, Valenzuela-Toro AM, Velez-Juarbe J, Santelli CM, Rubilar Rogers D, Cozzuol MA, Suárez M E. 2014. Repeated mass strandings of Miocene marine mammals from Atacama Region of Chile point to sudden death at sea. *Proceedings of the Royal Society B: Biological Sciences* **281**:20133316 DOI 10.1098/rspb.2013.3316.

Pyenson ND, Hoch E. 2007. Tortonian pontoporiid odontocetes from the eastern North Sea. *Journal of Vertebrate Paleontology* **27**:757–762 DOI 10.1671/0272-4634(2007)27[757:TPOFTE]2.0.CO;2.

Pyenson ND, Kelley NP, Parham JF. 2014. Marine tetrapod macroevolution: physical and biological drivers on 250 Ma of invasions and evolution in ocean ecosystems. *Palaeogeography, Palaeoclimatology, Palaeoecology* **400**:1–8 DOI 10.1016/j.palaeo.2014.02.018.

Pyenson ND, Sponberg SN. 2011. Reconstructing body size in extinct crown Cetacea (Neoceti) using allometry, phylogenetic methods and tests from the fossil record. *Journal of Mammalian Evolution* **18**:269–288 DOI 10.1007/s10914-011-9170-1.

Rensberger JM. 1969. A new iniid cetacean from the Miocene of California. *University of California Publications in Geological Sciences* **82**:1–34.

Robbins JA, Tao J, Grossman EL, O'Dea A. 2012. Exploring the delayed overturn in Caribbean fauna using gastropod stable-isotope profiles to quantify seasonal upwelling and freshening of coastal waters [Abstract 58-12]. *Geological Society of America Abstracts with Programs* **44(7)**:164.

Ruiz-Garcia M, Shostell JM. 2010. *Biology, evolution and conservation of river dolphins within South America and Asia*. Hauppauge: Nova Science Publishers, 1–504.

Salinas-Márquez, Fernando M, Barnes LG, Flores-Trujillo JG, Aranda-Manteca FJ. 2014. Una especie de delfín fósil (Cetacea; Delphinoidea; Kentriodontoidae) del Mioceno Medio de Baja California. *Boletín de la Sociedad Geológica Mexicana* **66**:145–164.

Scapino R. 1981. Morphological investigation into functions of the jaw symphysis in carnivorans. *Journal of Morphology* **167**:339–375 DOI 10.1002/jmor.1051670308.

Schusterman RJ, Kastak D, Levenson DH, Reichmuth CJ, Southall BL. 2000. Why pinnipeds don't echolocate. *The Journal of the Acoustical Society of America* **107**:2256–2264 DOI 10.1121/1.428506.

Schwarzhans W, Aguilera O. 2013. Otoliths of the Myctophidae from the Neogene of tropical America. *Palaeo Ichthyologica* **13**:83–150.

Secchi ER, Ott PH, Danilewicz DS. 2003. Effects of fishing by-catch and conservation status of the franciscana dolphin, *Pontoporia blainvillei*. In: Gales N, Hindell M, Kirkwood R, eds. *Marine mammals: fisheries, tourism and management issues*. Collingwood: CSIRO Publishing, 174–191.

Simpson GG. 1945. The principles of classification, and a classification of mammals. *Bulletin of the American Museum of Natural History* **85**:1–350.

Steeman ME, Hebsgaard MB, Fordyce RE, Ho SYW, Rabosky DL, Nielsen R, Rahbek C, Glenner H, Sørensen MV, Willerslev E. 2009. Radiation of extant cetaceans driven by restructuring of the oceans. *Systematic Biology* **58**:573–585 DOI 10.1093/sysbio/syp060.

Swofford DL. 2002. *PAUP* v.40b10*. Sunderland: Sinauer Associates.

Tanaka Y, Fordyce RE. 2014. Fossil dolphin *Otekaikea marplesi* (latest Oligocene, New Zealand) expands the morphological and taxonomic diversity of Oligocene cetaceans. *PLoS ONE* **9**:e107972 DOI 10.1371/journal.pone.0107972.

Tanaka Y, Fordyce RE. 2015. A new Oligo-Miocene dolphin from New Zealand: *Otekaikea huata* expands diversity of the early Platanistoidea. *Palaeontologia Electronica* **18.2.23A**:1–71.

Thewissen JG, Williams EM. 2002. The early radiations of Cetacea (Mammalia): evolutionary pattern and developmental correlations. *Annual Review of Ecology and Systematics* **33**:73–90 DOI 10.1146/annurev.ecolsys.33.020602.095426.

True FW. 1912. A fossil toothed cetacean from California representing a new genus and species. *Smithsonian Miscellaneous Collection* **60**:1–7.

Turvey ST, Barrett LA, Yujiang HAO, Lei Z, Xinqiao Z, Xianyan W, Yadong H, Kaiya Z, Hart T, Ding W. 2010. Rapidly shifting baselines in Yangtze fishing communities and local memory of extinct species. *Conservation Biology* **24**:778–787 DOI 10.1111/j.1523-1739.2009.01395.x.

Uhen MD. 2004. Form, function, and anatomy of *Dorudon atrox* (Mammalia, Cetacea): an archaeocete from the middle to late Eocene of Egypt. *University of Michigan Papers on Paleontology* **34**:1–222.

Uhen MD, Pyenson ND. 2007. Diversity estimates, biases, and historiographic effects: resolving cetacean diversity in the Tertiary. *Palaeontologia Electronica* **10**:11A–22.

Van Beneden P. 1864. Sur un Dauphin nouveau (*Delphinus guianensis*) et un Ziphioide rare. *Memoires de l'Academie Royale de Sciences Belgique, Bruxelles* **16**:1–21.

Velez-Juarbe J, Wood AR, De Gracia C, Hendy AJW. 2015. Evolutionary patterns among living and fossil kogiid sperm whales: evidence from the Neogene of Central America. *PLoS ONE* **10(5)**:e0129186 DOI 10.1371/journal.pone.0129186.

Vermeij GJ, Dudley R. 2000. Why are there so few evolutionary transitions between aquatic and terrestrial ecosystems? *Biological Journal of the Linnean Society* **70**:541–554 DOI 10.1111/j.1095-8312.2000.tb00216.x.

Vigil DI, Laurito CA. 2014. New fossil remains of an odontoceti (mammalia: Cetacea, physeteroidea) from the late miocene of Panama, Central America. *Revista Geológica de América Central* **50**:213–217.

Wade BS, Pearson PN, Berggren WA, Pälike H. 2011. Review and revision of Cenozoic tropical planktonic foraminiferal biostratigraphy and calibration to the geomagnetic polarity and astronomical time scale. *Earth-Science Reviews* **104**:111–142 DOI 10.1016/j.earscirev.2010.09.003.

Werth AJ. 2006. Mandibular and dental variation and the evolution of suction feeding in Odontoceti. *Journal of Mammalogy* **87**:579–588 DOI 10.1644/05-MAMM-A-279R1.1.

Whitmore Jr FC. 1994. Neogene climate change and the emergence of the modern whale fauna of the North Atlantic Ocean. In: Berta A, Deméré TA, eds. *Contributions in marine mammal paleontology Honoring Frank C. Whitmore, Jr*, *Proceedings of the San Diego society of natural history,* vol. 29. 223–228.

Zhou K, Zhou M, Zhao Z. 1984. First discovery of a Tertiary platanistoid fossil from Asia. *Scientific Reports of the Whales Research Institute, Toyko* **35**:173–181.